






Switched Command-Filtered-Based Adaptive Fuzzy Output-Feedback Funnel Control for Switched Nonlinear MIMO-Delayed Systems

Zhenhua Li , Hongtian Chen , Member, IEEE, Hak-Keung Lam , Fellow, IEEE, Wentao Wu , Student Member, IEEE, and Weidong Zhang , Senior Member, IEEE

Abstract—In this article, we consider the problem of switched-command-filtered-based adaptive fuzzy output-feedback funnel control for switched nonlinear multi-input multi-output (MIMO) delayed systems. A switched MIMO high-gain state observer is constructed for each subsystem to estimate unavailable system states. Compared with the conventional command filter technique, the main advantage is that the improved error-compensating signals are designed for each switched subsystem to remove the filtered errors and avoid an explosion of complexity and the singularity problem. Different from the traditional Lyapunov–Krasovskii functional method, design obstacles stemming from unknown time delays are overcome for the switched delayed systems by using appropriate multiple Lyapunov–Krasovskii functions and combining with the approximation capability of the fuzzy logic systems. Under a category of switching signals with mode-dependent average dwell time, all signals in the closed-loop switched system are semiglobally uniformly ultimately bounded under the output-feedback control; meanwhile, the tracking errors can remain in prespecified performance funnels. Case studies illustrate the flexibility and effectiveness of the proposed control approach.

Index Terms—Mode-dependent average dwell time (MDADT), multiple Lyapunov–Krasovskii functions, output-feedback fuzzy funnel control, switched command filter, switched nonlinear multi-input multi-output (MIMO) delayed systems.

Manuscript received 17 August 2023; revised 3 June 2024; accepted 21 July 2024. Date of current version 1 November 2024. This work was supported in part by the National Key R&D Program of China under Grant 2022ZD0119901, in part by the Shanghai Science and Technology Program under Grant 22015810300, in part by the National Natural Science Foundation of China under Grant 62303308 and Grant U2141234, in part by the Hainan Province Science and Technology Special Fund under Grant ZDYF2024GXJS003, in part by Shanghai Pujiang Program under Grant 23PJ1404700, in part by Joint Research Fund of Shanghai Academy of Spaceflight Technology under Grant USCAST2023-22, and in part by the Hainan Special Ph.D. Scientific Research Foundation of Sanya Yazhou Bay Science and Technology City under Grant HSPHDSRF-2022-01-005. Recommended by Associate Editor H. Gao. (Corresponding authors: Hongtian Chen; Weidong Zhang.)

Zhenhua Li is with the Department of Automation, Shanghai Jiao Tong University, Shanghai 200240, China, and also with the Hainan Research Institute, Shanghai Jiao Tong University, Sanya 572024, China (e-mail: lizhenhua@sjtu.edu.cn).

Hongtian Chen and Wentao Wu are with the Department of Automation, Shanghai Jiao Tong University, Shanghai 200240, China (e-mail: hongtian.chen@sjtu.edu.cn; wentao-wu@sjtu.edu.cn).

Hak-Keung Lam is with the Department of Engineering, King's College London, WC2R 2LS London, U.K. (e-mail: hak-keung.lam@kcl.ac.uk).

Weidong Zhang is with the Department of Automation, Shanghai Jiao Tong University, Shanghai 200240, China, and also with the School of Information and Communication Engineering, Hainan University, Haikou 570228, China (e-mail: wdzhang@sjtu.edu.cn).

Digital Object Identifier 10.1109/TFUZZ.2024.3434711

I. INTRODUCTION

SWITCHED systems, a common category of hybrid systems, have attracted much more attention over the last decades [1], [2], [3]. They consist of several subsystems and a switching signal, which can describe lots of practical systems, such as single-link robots, inverted pendulums, data communication networks, and chemical reactor systems [4], [5], [6], [7]. One key issue in the study of switched systems is the design of a proper switching signal. Up to now, some significant design methods for switched systems have been reported, such as the multiple Lyapunov functions, common Lyapunov function, dwell time, average dwell time, mode-dependent average dwell time (MDADT) [7], [8], [9], [10], [11], [12]. Meanwhile, it is worth noting in [11] that MDADT-based switching is more general since both dwell time and average dwell time are considered special switching cases. In the practical application of switched systems, it is unavoidable to suffer from time delays due to data transmission, self-physical characteristics, etc. In general, the Lyapunov–Razumikhin and the Lyapunov–Krasovskii functional methods are popular in addressing the delayed systems [13], [14]. It is often the case that time delays adversely affect the system control performance. Otherwise, they can even result in the instabilities of existing control systems. Therefore, it is expected to develop control strategies with MDADT-based switching for the switched nonlinear delayed systems.

Especially, the backstepping technique is an effective control design approach for nonswitched or switched delayed nonlinear systems. In the traditional backstepping technique, the explosion of dimensionality, also called the explosion of complexity, arises from the repeated differentiation of certain nonlinear functions, such as virtual controllers. This process inevitably leads to a more complicated algorithm with a heavy computational burden, which becomes significantly more pronounced as the order of system increases. Meanwhile, the singularity problem, which can arise when differentiating the virtual control law as indicated in [1] and [15], may lead to the instability of the nonlinear systems. To address this issue, Swaroop et al. [16] presented a dynamic surface control technique. In adaptive control, fuzzy logic systems are one of the most popular adaptive tools via the dynamic surface control technique to address the issue for the nonswitched or switched nonlinear systems [17], [18], [19], [20]. In fact, these adaptive dynamic surface control strategies

with fuzzy logic systems have ignored the effect caused by filtering errors in the control systems. To deal with this problem, a novel command filter was presented to replace the first-order filter in the dynamic surface control design. Thus, the command filter technique has received great attention in the control design for nonlinear systems [21], [22], [23]. Then, this method has also been developed for the adaptive control design for the switched nonlinear systems, such as event-triggered mechanism with the common Lyapunov function method [24], the finite-time tracking control under state-dependent switching [8], and time-schedule Lyapunov function under asynchronous switching [12]. However, the switched command filter does not consider the transient and steady-state control performance of the switched nonlinear delayed systems with these adaptive intelligent control strategies.

Moreover, other studies have focused on performance-related control requirements for the nonlinear systems [25], [26]. Based on the transient and steady-state performance requirements, the prescribed control performance control was presented for the feedback linearizable multi-input multi-output (MIMO) nonlinear systems in [27]. In the prescribed performance control, a performance-oriented objective function is used to change the tracking error of the original system into a new error system under state transformation. The prescribed performance control scheme was successfully employed in the adaptive control design for stochastic nonlinear systems [28], MIMO nonlinear systems [26], etc. However, the conventional prescribed performance control may cause instability because of its singularity. Meanwhile, the funnel control was first proposed by Ilchmann et al. [29], which was also applied to enhance these requirements of the control systems. The nonlinear systems under the funnel control work well without a prior about the plants with measurement noises and parameter uncertainties. In [30], an adaptive fuzzy funnel controller was developed for nonlinear nonaffine systems using the backstepping method in the finite time. The funnel control strategy has been successfully developed for stability and stabilization of non-switched or switched nonlinear systems [25], [30]. However, due to the limited measurement of system states, no study has also been reported on the adaptive fuzzy output-feedback funnel control with a switched command filter for switched nonlinear MIMO-delayed systems under a category of switching signals with MDADT.

Motivated by the above discussions, this study focuses on the adaptive fuzzy output feedback funnel control with a switched command filter for switched nonlinear MIMO-delayed systems. The main contributions of this study are summarized as follows.

- 1) The adaptive fuzzy output-feedback funnel tracking control scheme is flexibly presented for the switched nonlinear MIMO-delayed systems using the multiple Lyapunov–Krasovskii functions under a category of switching signals with MDADT.
- 2) To deal with the explosion of dimensionality in the backstepping technique, a novel switched command filter is constructed for each switched subsystem without the potential singularity problem, where the compensation signals are presented to decrease the influence of the errors produced from the filter.

- 3) Due to the absence of measurements, the adaptive fuzzy output feedback controllers are implemented for each subsystem with the switched high-gain state observer, such that the tracking errors can remain in the prespecified performance funnels.

The rest of this article is organized as follows. Section II mainly includes the system description. The controller scheme and stability analysis are presented in Section III. Section IV shows the effectiveness and flexibility of the proposed control strategy. Finally, Section V concludes this article.

II. SYSTEM DESCRIPTION

A. Switched Nonlinear MIMO-Delayed Systems

Consider the switched nonlinear MIMO-delayed systems in the following nonstrict-feedback form:

$$\dot{x}_{il} = x_{i,l+1} + f_{il\sigma(t)}(x) + h_{il\sigma(t)}(x_\tau) \quad (1a)$$

$$\dot{x}_{im} = u_{i\sigma(t)} + f_{im\sigma(t)}(x) + h_{im\sigma(t)}(x_\tau) \quad (1b)$$

$$y_i = x_{i1} \quad (1c)$$

where $l = 1, \dots, m-1$ and $x_i = [x_{i1}, \dots, x_{im}]^\top \in \mathbb{R}^m$ is the system state with $x = [x_1^\top, \dots, x_n^\top]^\top \in \mathbb{R}^{n \times m}$. The switched systems (1) consist of n interconnected subsystems \mathbb{N}_i for $i = 1, \dots, n$. A switching signal $\sigma(t)$ is a piecewise right continuous function with $M \geq 2$ being the number of subsystems satisfying $\sigma(t) : [0, \infty) \rightarrow \mathbb{M} = \{1, \dots, M\}$. Note that during $t \in [t_j, t_{j+1})$, one gets $\sigma(t) = k \in \mathbb{M}$, where t_j and t_{j+1} are the time instant. The control input of the k th subsystem is described by $u_k = [u_{1k}, \dots, u_{nk}]^\top \in \mathbb{R}^n$. $y = [y_1, \dots, y_n]^\top \in \mathbb{R}^n$ is the system output. For $k \in \mathbb{M}$ and $l = 1, \dots, m$, $f_{ilk}(\cdot) \in \mathbb{R}$ and $h_{ilk}(\cdot) \in \mathbb{R}$ are the unknown continuous nonlinear functions. For known constants $\tau > 0$ and $\bar{\tau} > 0$, the delayed state x_τ is defined as $x_\tau = [x_{1\tau}^\top, \dots, x_{n\tau}^\top]^\top \in \mathbb{R}^{n \times m}$ with $x_{i\tau} = x_i(t - \tau_i(t))$ and $x_{ij\tau} = x_{ij}(t - \tau_i(t))$ for $i = 1, \dots, n$ and $j = 1, \dots, m$, where $\tau_i(t)$ is the unknown time-varying delay with $0 < \tau_i(t) \leq \tau$ and $\dot{\tau}_i(t) \leq \bar{\tau} < 1$. In this case, $\Upsilon(t_0) = x(t_0) \in \mathbb{R}^{n \times m}$ represents the initial vector at $t_0 \in [-\tau, 0]$.

Definition 1 (See [11]): For the switched systems, a switching signal $\sigma(t)$ satisfying an MDADT $\tau_{ak} > 0$ holds that

$$N_{\sigma k}(T, t) \leq N_{0k} + \frac{T_k(T, t)}{\tau_{ak}} \quad \forall T \geq t \geq 0 \quad (2)$$

where $N_{\sigma k}(T, t)$ stands for the switching numbers on the interval $[t, T]$ if the k th subsystem is active, $T_k(T, t)$ represents the whole running time of the k th subsystem on the interval $[t, T]$, and $N_{0k} > 0$ is called the mode-dependent chatter bounds.

The control objective is to construct a switched command-filtered-based adaptive fuzzy output-feedback funnel controllers of subsystems for the switched nonlinear MIMO-delayed systems based on the multiple Lyapunov–Krasovskii functions such that

- 1) all the closed-loop signals achieve semi-globally uniformly ultimate bounded under a category of switching signals with MDADT for any bounded initial conditions, and

- 2) the tracking errors $y_i - y_{ir}$ for $i = 1, 2, \dots, n$ converge to the prespecified performance funnels under the given reference signals y_{ir} .

Assumption 1: For $i = 1, \dots, n$, $l = 1, \dots, m$, and $k \in \mathbb{M}$, the nonlinear functions $f_{ilk}(\cdot)$ and $h_{ilk}(\cdot)$ can satisfy the following inequalities $f_{ilk}^2(x) \leq \sum_{j=1}^n F_{ilj}^2(x_j)$, $h_{ilk}^2(x_\tau) \leq \sum_{j=1}^n H_{ilj}^2(x_{j\tau})$, where F_{ilj} and H_{ilj} are unknown nonnegative smooth functions satisfying $F_{ilj}(0) = 0$ and $H_{ilj}(0) = 0$.

Assumption 2: The reference signals $y_{ir}(t)$ for $i = 1, 2, \dots, n$ and their derivatives $y_{ir}^{(1)}(t), \dots, y_{ir}^{(n)}(t)$ are continuous and bounded.

Remark 1: Assumption 1 is a general assumption that is used to deal with the nonlinear time-delay terms. In fact, for any continuous function $h_{ilk}(x_{1\tau}, \dots, x_{n\tau}) : \mathbb{R}^{n \times m} \rightarrow \mathbb{R}$, there exist positive smooth functions $H_{il1}(x_{1\tau}), \dots, H_{iln}(x_{n\tau})$ such that $|h_{ilk}(x_\tau)| \leq \sum_{j=1}^n H_{ilj}(x_{j\tau})$, i.e., $h_{ilk}^2(x_\tau) \leq \sum_{j=1}^n H_{ilj}^2(x_{j\tau})$, which can be commonly found, such as in [7] and [10].

B. Fuzzy Logic Systems

Fuzzy logic systems are one of the most popular approaches to approximate unknown nonlinear continuous functions. The knowledge base for the fuzzy logic system concludes a collection of fuzzy IF-THEN rules described as R^i : If \bar{x}_1 is F_1^i , \bar{x}_2 is F_2^i , ..., and \bar{x}_n is F_n^i , then \bar{y} is G^i , $i = 1, \dots, \ell$, where $\bar{x} = [\bar{x}_1, \dots, \bar{x}_n]^\top$ and \bar{y} are the input and output of the fuzzy logic system, respectively. F_m^i for $m = 1, \dots, n$ and G^i are the fuzzy sets. ℓ is the number of rules. According to [6] and [31], the fuzzy logic system can be defined as $\bar{y}(\bar{x}) = \sum_{i=1}^{\ell} \bar{y}_i \prod_{m=1}^n \mu_{F_m^i}(\bar{x}_m) / \sum_{i=1}^{\ell} [\prod_{m=1}^n \mu_{F_m^i}(\bar{x}_m)]$, where $\bar{y}_i = \max_{y \in \mathbb{R}} \mu_{G^i}(y)$. $\mu_{F_m^i}(\bar{x}_m)$ and $\mu_{G^i}(\bar{y})$ are the fuzzy membership functions of F_m^i and G^i , respectively. Meanwhile, the fuzzy basic functions are denoted as $s_i(\bar{x}) = \prod_{m=1}^n \mu_{F_m^i}(\bar{x}_m) / \sum_{i=1}^{\ell} [\prod_{m=1}^n \mu_{F_m^i}(\bar{x}_m)]$. Define $W^\top = [\bar{y}_1, \bar{y}_2, \dots, \bar{y}_\ell] = [W_1, W_2, \dots, W_\ell]$ and $S(\bar{x}) = [s_1(\bar{x}), \dots, s_\ell(\bar{x})]^\top$. Finally, the fuzzy logic system can be described as $\bar{y}(\bar{x}) = W^\top S(\bar{x})$.

Lemma 1 (See [1], [32]): If the function $\bar{f}(\bar{x})$ is continuous and defined on a compact set Ω , then, for any positive constant ϑ , a fuzzy logic system exists and satisfies $\sup_{\bar{x} \in \Omega} |\bar{f}(\bar{x}) - W^\top S(\bar{x})| \leq \vartheta$.

Based on Lemma 1, the continuous function $\bar{f}(\bar{x})$ can be denoted as

$$\bar{f}(\bar{x}) = W^{*\top} S(\bar{x}) + \delta(\bar{x}) \quad (3)$$

where W^* demonstrates an ideal weight vector. $\delta(\bar{x})$ is the error of approximation satisfying $|\delta(\bar{x})| \leq \delta^*$ with any given positive constant δ^* . For convenience, $\bar{f}(\bar{x})$ is described as $\bar{f}(\bar{x}) = W^{*\top} S + \delta$ with

$$W^* = \arg \min_{W \in \mathbb{R}^\ell} \left\{ \sup_{\bar{x} \in \Omega} |\bar{f}(\bar{x}) - W^\top S(\bar{x})| \right\}. \quad (4)$$

C. Funnel Control

The funnel control technique is utilized to deal with the problem of the system control performance in [29].

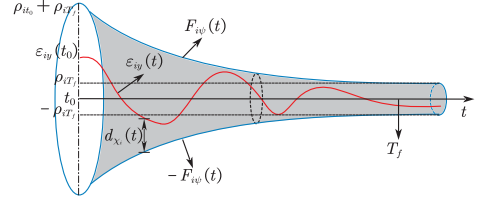


Fig. 1. Schematic of the funnel control performance.

For $i = 1, 2, \dots, n$, the funnel controller is denoted as $u_i(t) = \Xi_i(F_{i\psi}(t), \chi_i(t), \|\varepsilon_{iy}(t)\|)\varepsilon_{iy}(t)$, where $\varepsilon_{iy}(t) = y_i(t) - y_{ir}(t)$ is the tracking error, $F_{i\psi}(t)$ is the boundary of the funnel, $\chi_i(t)$ is the scaling function, and $\Xi_i(t)$ is a time-varying gain.

Let $\psi_i(t)$ be a continuous and bounded function satisfying $\psi_i(t) > 0, \forall t \geq 0$, and $\sup_{t \geq 0} \psi_i(t) < \infty$. Then, $F_{i\psi}(t)$ is denoted as the reciprocal of $\psi_i(t)$. To proceed, the funnel $F_{i\psi}(t)$ belongs to the following compact set $F_{i\psi}(t) = \{(t, \varepsilon_{iy}) \in \mathbb{R} \times \mathbb{R}^m \mid \psi_i(t)\|\varepsilon_{iy}(t)\| < 1\}$. In addition, define the vertical distance $d_{\chi_i}(t)$ as $d_{\chi_i}(t) = F_{i\psi}(t) - \|\varepsilon_{iy}(t)\|$. The adjustable gain $\Xi_i(t)$ is denoted as $\Xi_i(t) = \chi_i(t)/d_{\chi_i}(t)$. If the tracking error $\varepsilon_{iy}(t)$ tends to the boundary $F_{i\psi}(t)$, then the gain $\Xi_i(t)$ will increase. Conversely, the gain $\Xi_i(t)$ will decrease if the tracking error $\varepsilon_{iy}(t)$ is far from the boundary $F_{i\psi}(t)$. Based on [25], $F_{i\psi}(t)$ is considered as follows:

$$F_{i\psi}(t) = \begin{cases} \left(\rho_{it_0} - \frac{t}{T_f}\right) e^{\left(1 - \frac{T_f}{T_f - t}\right)} + \rho_{iT_f}, & t \in [t_0, T_f) \\ \rho_{iT_f}, & t \in [T_f, +\infty) \end{cases} \quad (5)$$

where for $i = 1, 2, \dots, n$, $\rho_{it_0} \geq 1, \rho_{iT_f} > 0$, and $T_f > 0$ are the design constants. If the initial time is $t_0 = 0$, then $F_{i\psi}(t_0) = \rho_{it_0} + \rho_{iT_f}$ holds satisfying $\|\varepsilon_{iy}(t_0)\| < F_{i\psi}(t_0)$. To proceed, $F_{i\psi}(t)$ approaches ρ_{iT_f} in a finite time T_f (see Fig. 1 for details). Thus, a state transformation for a funnel error is denoted as

$$z_{i1} = \frac{\varepsilon_{iy}}{\sqrt{F_{i\psi}^2 - \varepsilon_{iy}^2}} \quad (6)$$

whose time derivative from (1) can be obtained as

$$\dot{z}_{i1} = \Gamma_{i1} \left(\dot{x}_{i1} - \dot{y}_{ir} - \frac{\varepsilon_{iy} \dot{F}_{i\psi}}{F_{i\psi}} \right) \quad (7)$$

where $\Gamma_{i1} = F_{i\psi}^2 / (F_{i\psi}^2 - \varepsilon_{iy}^2)^{\frac{3}{2}}$ is a positive function. The flowchart of the funnel control is shown in Fig. 2.

Remark 2: In the referenced paper by Han and Lee [33], a funnel error surface is given as $\zeta(t) = \frac{e(t)}{F_{i\psi}(t) - \|e(t)\|}$. It is noteworthy that $\zeta(t)$ fails to be differentiable at the point $e(t) = 0$, which does not align with the differentiability requirement of backstepping techniques. This nondifferentiability may pose challenges when integrating the funnel variable ξ_1 within backstepping control frameworks. Unlike the nonsingular finite-time sliding mode control [34], our funnel error surface does not explicitly guarantee finite-time convergence to the origin in a finite time T_f . Instead, it ensures that the error remains within

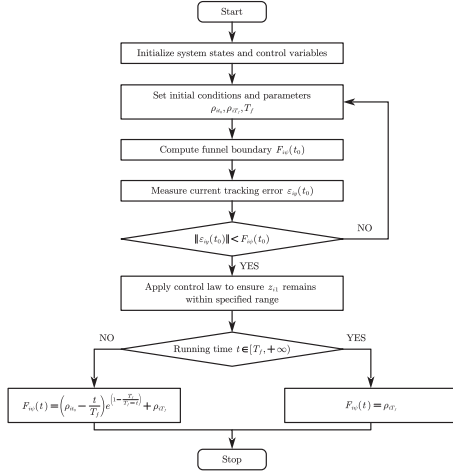


Fig. 2. Flowchart of the funnel control.

a progressively narrowing funnel boundary, providing a form of asymptotic performance rather than finite-time convergence.

III. MAIN RESULTS

By employing the multiple Lyapunov–Krasovskii functions, this section will develop a switched-command-filtered-based adaptive fuzzy output-feedback funnel control scheme for the switched system (1) in the constructive design via the backstepping method. The analysis of stability will be shown in the closed-loop switched system under MDADT.

A. Switched High-Gain MIMO State Observer Design

To estimate the unavailable states, a switched high-gain MIMO state observer is considered as

$$\dot{\hat{x}}_{il} = \hat{x}_{i,l+1} + L_{il\sigma(t)}(y_i - \hat{x}_{i1}) \quad (8a)$$

$$\dot{\hat{x}}_{im} = u_{i\sigma(t)} + L_{im\sigma(t)}(y_i - \hat{x}_{i1}) \quad (8b)$$

where $l = 1, \dots, m-1$, $\sigma(t)$ is the same switching signal as described in (1), and \hat{x}_{il} for $l = 1, 2, \dots, m$ is the estimate of the system state x_{il} . For $k \in \mathbb{M}$ and $l = 1, 2, \dots, m$, L_{ilk} denote positive constants to be designed, such that the following Hurwitz matrices hold:

$$A_{ik} = \begin{bmatrix} -L_{i1k} & & \\ & \ddots & I_{m-1} \\ -L_{imk} & 0 \cdots 0 \end{bmatrix}.$$

where I_{m-1} is an $(m-1)$ -dimension identity matrix. In other words, for definite symmetric matrices Q_{ik} , the symmetric definite matrices P_{ik} exists and satisfies

$$A_{ik}^\top P_{ik} + P_{ik} A_{ik} = -Q_{ik}. \quad (9)$$

Let the error of the state observer be

$$\varepsilon_i = [\varepsilon_{i1}, \dots, \varepsilon_{im}]^\top = x_i - \hat{x}_i \in \mathbb{R}^m \quad (10)$$

where $\hat{x}_i = [\hat{x}_{i1}, \dots, \hat{x}_{im}]^\top$ is the estimation of the system state x_i for $i = 1, \dots, n$. To proceed, combining (1) with (8), one gets

$$\dot{\varepsilon}_i = A_{ik}\varepsilon_i + f_{ik}(x) + h_{ik}(x_\tau), \quad k \in \mathbb{M} \quad (11)$$

where $f_{i,k} = [f_{i1k}, \dots, f_{imk}]^\top \in \mathbb{R}^m$ and $h_{i,k} = [h_{i1k}, \dots, h_{imk}]^\top \in \mathbb{R}^m$. As a matter of convenience, the unknown ideal values are expressed as

$$\theta_{il}^* = \max \{ \|W_{ilk}^*\|, k \in \mathbb{M} \} \quad (12)$$

where $l = 0, 1, \dots, m$, W_{ilk}^* stands for the ideal constant weight vector. Meanwhile, $\hat{\theta}_{il}$ is the estimation error satisfying $\hat{\theta}_{il} = \theta_{il}^* - \hat{\theta}_{il}$, and $\hat{\theta}_{il}$ is the estimation of θ_{il}^* . The following lemma is provided first to facilitate the proof of the main theorem.

Lemma 2: For the observer error system (11), let the Lyapunov function candidate be

$$V_{i0k} = \varrho_i \varepsilon_i^\top P_{ik} \varepsilon_i, \quad i = 1, \dots, n, \quad k \in \mathbb{M}. \quad (13)$$

Then, \dot{V}_{i0k} satisfies

$$\begin{aligned} \dot{V}_{i0k} &\leq -\varrho_i (\underline{\lambda}(Q_{ik}) - 2r_{i0}e^{\beta\tau}) \|\varepsilon_i\|^2 + \Theta_{i0k} - \bar{f}_{i0k}(X_0) \\ &\quad + \frac{\varrho_i e^{-\beta\tau}}{r_{i0}} \|P_{ik}\|^2 \sum_{l=1}^m \sum_{j=1}^n (F_{ilj}^2(x_j) + H_{ilj}^2(x_{j\tau})) \end{aligned} \quad (14)$$

where ϱ_i is a positive parameter, $\underline{\lambda}(Q_{ik})$ stands for the smallest eigenvalue of the matrix Q_{ik} , and Θ_{i0k} is an unknown constant with $\Theta_{i0k} = \theta_{i0}^* + \delta_{i0}^*$.

Proof: By using (9) and (11), one gets \dot{V}_{i0k} satisfied by

$$\dot{V}_{i0k} = -\varrho_i \varepsilon_i^\top Q_{ik} \varepsilon_i + 2\varrho_i \varepsilon_i^\top P_{ik} (f_{ik}(x) + h_{ik}(x_\tau)). \quad (15)$$

In what follows, the inequalities are determined by the definition of Young's inequality

$$\begin{aligned} 2\varrho_i \varepsilon_i^\top P_{ik} f_{ik}(x) &\leq \varrho_i r_{i0} e^{\beta\tau} \|\varepsilon_i\|^2 \\ &\quad + \frac{\varrho_i e^{-\beta\tau}}{r_{i0}} \|P_{ik}\|^2 \sum_{l=1}^m \sum_{j=1}^n F_{ilj}^2(x_j) \end{aligned} \quad (16)$$

$$\begin{aligned} 2\varrho_i \varepsilon_i^\top P_{ik} h_{ik}(x_\tau) &\leq \varrho_i r_{i0} e^{\beta\tau} \|\varepsilon_i\|^2 \\ &\quad + \frac{\varrho_i e^{-\beta\tau}}{r_{i0}} \|P_{ik}\|^2 \sum_{l=1}^m \sum_{j=1}^n H_{ilj}^2(x_{j\tau}) \end{aligned} \quad (17)$$

where β and r_{i0} are the positive parameters. Suppose that the unknown continuous function is $\bar{f}_{i0k}(X_{i0})$. Further, combining (3), (12), and Lemma 1 yields

$$\bar{f}_{i0k}(X_{i0}) \leq \|W_{i0k}^* S_{i0}(X_{i0})\| + |\delta_{i0k}| \leq \theta_{i0}^* + \delta_{i0}^*. \quad (18)$$

Then, substituting (16)–(18) into (15), one gets (14). The proof of Lemma 2 has been completed. ■

B. Design of Output-Feedback Funnel Controllers

For system (1), define the following coordinate transformation:

$$z_{il} = \hat{x}_{il} - \bar{\alpha}_{il}(\cdot), \quad l = 2, \dots, m \quad (19)$$

where $\bar{\alpha}_{il}(\cdot)$ is the output of switched command filter. The adaptive backstepping control design is based on (6) and (19). Inspired by [35], the switched command filter is designed as

$$\dot{\varphi}_{il1} = \varpi_{ik} \varphi_{il2} \quad (20a)$$

$$\dot{\varphi}_{il2} = -2\zeta_{ik} \varpi_{ik} \varphi_{il2} - \varpi_{ik} (\varphi_{il1} - \alpha_{il}) \quad (20b)$$

where $\bar{\alpha}_{i,l+1} = \varphi_{il1}$, α_{il} is the input of the filter for $l = 1, 2, \dots, m-1$, ϖ_{ik} and ζ_{ik} for $k \in \mathbb{M}$ are the positive constants satisfying $\zeta_{ik} \in (0, 1]$.

To compensate for the error produced from $\bar{\alpha}_{i,l+1}$ and α_{il} for $i = 1, \dots, n$ and $l = 1, \dots, m-1$, the compensating signals ξ_{il} for $l = 1, \dots, m$ are designed as

$$\dot{\xi}_{i1} = -\bar{c}_{i1}\xi_{i1} + \Gamma_{i1}(\xi_{i2} + \bar{\alpha}_{i2} - \alpha_{i1} - d_{i1}\text{sign}(\xi_{i1})) \quad (21a)$$

$$\begin{aligned} \dot{\xi}_{i2} = & -\bar{c}_{i2}\xi_{i2} - \Gamma_{i1}\xi_{i,1} + \xi_{i,3} + \bar{\alpha}_{i,3} \\ & - \alpha_{i2} - d_{i2}\text{sign}(\xi_{i2}) \end{aligned} \quad (21b)$$

$$\begin{aligned} \dot{\xi}_{il} = & -\bar{c}_{il}\xi_{il} - \xi_{i,l-1} + \xi_{i,l+1} + \bar{\alpha}_{i,l+1} \\ & - \alpha_{il} - d_{il}\text{sign}(\xi_{il}), \quad l = 3, \dots, n-1 \end{aligned} \quad (21c)$$

$$\dot{\xi}_{im} = -\bar{c}_{im}\xi_{im} - \xi_{i,m-1} \quad (21d)$$

where \bar{c}_{il} , \bar{c}_{imk} , and d_{il} are some positive constants for $i = 1, \dots, n$, $k \in \mathbb{M}$, and $l = 1, \dots, m-1$. To proceed, define the error variables of compensating signals as

$$\omega_{il} = z_{il} - \xi_{il}, \quad l = 1, \dots, m. \quad (22)$$

The detailed design process of the control scheme is shown in the following steps.

Initial step: Based on (7) and (22), the dynamics of ω_{i1} can be obtained as follows:

$$\dot{\omega}_{i1} = \Gamma_{i1} \left(\dot{x}_{i1} - \dot{y}_{ir} - \frac{\varepsilon_{iy}\dot{F}_{i\psi}}{F_{i\psi}} \right) - \dot{\xi}_{i1}. \quad (23)$$

Construct the Lyapunov function candidate as

$$V_{i1k} = V_{i0k} + \frac{1}{2}\omega_{i1}^2 + \frac{1}{2\ell_{i1}}\tilde{\theta}_{i1}^2, \quad k \in \mathbb{M} \quad (24)$$

where ℓ_{i1} is a positive constant. To proceed, based on (1), (10), (23), and (24), one gets

$$\begin{aligned} \dot{V}_{i1k} &= \dot{V}_{i0k} - \frac{1}{\ell_{i1}}\tilde{\theta}_{i1}\dot{\tilde{\theta}}_{i1} + \Gamma_{i1}\omega_{i1} \left[\omega_{i2} + \xi_{i2} + \bar{\alpha}_{i2} + \varepsilon_{i2} - \dot{y}_{ir} \right. \\ &\quad \left. + f_{i1k}(x) + h_{i1k}(x_\tau) - \frac{\varepsilon_{iy}\dot{F}_{i\psi}}{F_{i\psi}} \right] - \omega_{i1}\dot{\xi}_{i1}. \end{aligned} \quad (25)$$

By utilizing Young's inequality, one has

$$\Gamma_{i1}\omega_{i1}\varepsilon_{i2} \leq \frac{e^{-\beta\tau}}{4\varrho_{i1}r_{i0}}\Gamma_{i1}^2\omega_{i1}^2 + \varrho_{i1}r_{i0}e^{\beta\tau}\|\varepsilon_i\|^2 \quad (26)$$

$$\Gamma_{i1}\omega_{i1}f_{i1k}(x) \leq \frac{r_{i1}e^{\beta\tau}}{2}\Gamma_{i1}^2\omega_{i1}^2 + \frac{e^{-\beta\tau}}{2r_{i1}}\sum_{j=1}^n F_{i1j}^2(x_j) \quad (27)$$

$$\Gamma_{i1}\omega_{i1}h_{i1k}(x_\tau) \leq \frac{r_{i1}e^{\beta\tau}}{2}\Gamma_{i1}^2\omega_{i1}^2 + \frac{e^{-\beta\tau}}{2r_{i1}}\sum_{j=1}^n H_{i1j}^2(x_{j\tau}) \quad (28)$$

$$\Gamma_{i1}\omega_{i1}d_{i1}\text{sign}(\xi_{i1}) \leq r_{i1}e^{\beta\tau}\Gamma_{i1}^2\omega_{i1}^2 + \frac{e^{-\beta\tau}}{4r_{i1}}d_{i1}^2 \quad (29)$$

where r_{i1} is a positive parameter. Then, $\bar{f}_{i1}(X_{i1}) = (\frac{e^{-\beta\tau}}{4\varrho_{i1}r_{i0}} + 2r_{i1}e^{\beta\tau})\Gamma_{i1}^2\omega_{i1} - \Gamma_{i1}(\dot{y}_{ir} + \frac{\varepsilon_{iy}\dot{F}_{i\psi}}{F_{i\psi}})$ is denoted as the uncertain

continuous function with $X_{i1} = [\omega_{i1}, x_{i1}, y_{ir}, \dot{y}_{ir}]^\top$. Based on (3) and (4), a fuzzy logic system is introduced as

$$\bar{f}_{i1k}(X_{i1}) = W_{i1k}^{*\top}S_{i1} + \delta_{i1k} \quad (30)$$

where δ_{i1k} is the approximation error with $|\delta_{i1k}| < \delta_{i1}^*$ and δ_{i1}^* is a positive parameter. Based on (12), (30), and Lemma 1, one gets

$$\begin{aligned} \omega_{i1}\bar{f}_{i1k}(X_{i1}) &= \omega_{i1}W_{i1k}^{*\top}S_{i1} + \omega_{i1}\delta_{i1k} \\ &\leq \frac{1}{2a_{i1}^2}\omega_{i1}^2\theta_{i1}^*S_{i1}^\top S_{i1} + \frac{1}{2}a_{i1}^2 + \frac{1}{2}\omega_{i1}^2 + \frac{1}{2}\delta_{i1}^{*2} \end{aligned} \quad (31)$$

where a_{i1} is a positive constant. Then, the virtual controller input α_{i1} and the adaptive law $\hat{\theta}_{i1}$ are considered as

$$\alpha_{i1} = -\Gamma_{i1}^{-1} \left[\bar{c}_{i1}z_{i1} + \frac{1}{2a_{i1}^2}\omega_{i1}\hat{\theta}_{i1}S_{i1}^\top S_{i1} \right] \quad (32)$$

$$\dot{\hat{\theta}}_{i1} = \frac{\ell_{i1}}{2a_{i1}^2}\omega_{i1}^2S_{i1}^\top S_{i1} - \gamma_{i1}\hat{\theta}_{i1} \quad (33)$$

where γ_{i1} is a positive parameter. Combining (25)–(33) induces

$$\begin{aligned} \dot{V}_{i1k} \leq & -\varrho_i(\lambda(Q_{ik}) - 3r_{i0}e^{\beta\tau})\|\varepsilon_i\|^2 + \frac{\gamma_{i1}}{\ell_{i1}}\tilde{\theta}_{i1}\hat{\theta}_{i1} \\ & - c_{i1}\omega_{i1}^2 + \Gamma_{i1}\omega_{i1}\omega_{i2} + \Theta_{i1k} - \bar{f}_{i0k}(X_0) \\ & + \frac{\varrho_i e^{-\beta\tau}}{r_0}\|P_{ik}\|^2 \sum_{l=1}^m \sum_{j=1}^n (F_{ilj}^2(x_j) + H_{ilj}^2(x_{j\tau})) \\ & + \frac{e^{-\beta\tau}}{2r_{i1}} \sum_{j=1}^n (F_{i1j}^2(x_j) + H_{i1j}^2(x_{j\tau})) \end{aligned} \quad (34)$$

where $c_{i1} = \bar{c}_{i1} - \frac{1}{2}$ and $\Theta_{i1k} = \Theta_{i0k} + \frac{e^{-\beta\tau}}{4r_{i1}}d_{i1}^2 + \frac{1}{2}a_{i1}^2 + \frac{1}{2}\delta_{i1}^{*2}$.

Inductive Step ($2 \leq l \leq m-1$): Based on (8), (19), and (22), one gets the following dynamics of ω_{il} as

$$\dot{\omega}_{il} = z_{i,l+1} + \bar{\alpha}_{i,l+1} + L_{ilk}\varepsilon_{i1} - \dot{\alpha}_{il} - \dot{\xi}_{il}.$$

The Lyapunov function can be constructed by

$$V_{ilk} = V_{i,l-1,k} + \frac{1}{2}\omega_{il}^2 + \frac{1}{2\ell_{il}}\tilde{\theta}_{il}^2 \quad (35)$$

where ℓ_{il} is a positive constant. Furthermore, it is deduced that

$$\begin{aligned} \dot{V}_{ilk} &= \omega_{il}[\omega_{i,l+1} + L_{ilk}\varepsilon_{i1} + \xi_{i,l+1} + \bar{\alpha}_{i,l+1} - \dot{\alpha}_{il} - \dot{\xi}_{il}] \\ &\quad + \dot{V}_{i,l-1,k} - \frac{1}{\ell_{il}}\tilde{\theta}_{il}\dot{\tilde{\theta}}_{il}. \end{aligned} \quad (36)$$

Utilizing Young's inequality, one has

$$\omega_{il}d_{il}\text{sign}(\xi_{il}) \leq r_{il}e^{\beta\tau}\omega_{il}^2 + \frac{e^{-\beta\tau}}{4r_{il}}d_{il}^2 \quad (37)$$

where r_{il} is a positive parameter. Similar to the initial step, the uncertain functions are considered as $\bar{f}_{ilk}(X_{il}) = L_{ilk}\varepsilon_{i1} - \dot{\alpha}_{il} + r_{il}e^{\beta\tau}\omega_{il}$ with $X_{il} = [x_{i1}, y_{ir}, y_{ir}^{(1)}, \dots, y_{ir}^{(l-1)}, \hat{\theta}_{i1}, \dots, \hat{\theta}_{i,l-1}, \hat{x}_{i1}, \dots, \hat{x}_{il}, \omega_{i1}, \dots, \omega_{il}]^\top$. Based on (3) and (4), the uncertain functions $\bar{f}_{ilk}(X_{il})$ also can be determined by a fuzzy logic system satisfying

$$\bar{f}_{ilk}(X_{il}) = W_{ilk}^{*\top}S_{il} + \delta_{ilk} \quad (38)$$

where the error of approximation δ_{ilk} is satisfied by $|\delta_{ilk}| < \delta_{il}^*$ with a positive parameter δ_{il}^* . Based on Lemma 1, Young's inequality, (12), and (38), one has

$$\begin{aligned} \omega_{il} \bar{f}_{ilk}(X_{il}) &= \omega_{il} W_{ilk}^{*\top} S_{il} + \omega_{il} \delta_{ilk} \\ &\leq \frac{1}{2a_{il}^2} \omega_{il}^2 \theta_{il}^* S_{il}^\top S_{il} + \frac{1}{2} a_{il}^2 + \frac{1}{2} \omega_{il}^2 + \frac{1}{2} \delta_{il}^{*2} \end{aligned} \quad (39)$$

where a_{il} is a positive designed parameter. Meanwhile, the virtual controller input α_{il} and the adaptive laws $\hat{\theta}_{il}$ can be considered as

$$\alpha_{il} = -\bar{c}_{il} z_{il} - z_{i,l-1} - \frac{1}{2a_{il}^2} \omega_{il} \hat{\theta}_{il} S_{il}^\top S_{il} \quad (40)$$

$$\dot{\hat{\theta}}_{il} = \frac{\ell_{il}}{2a_{il}^2} \omega_{il}^2 S_{il}^\top S_{il} - \gamma_{il} \hat{\theta}_{il} \quad (41)$$

where γ_{il} is a positive constant, and $\alpha_{i2} = -\bar{c}_{i2} z_{i2} - \Gamma_{i1} z_{i,1} - \frac{1}{2a_{i2}^2} \omega_{i2} \hat{\theta}_{i2} S_{i2}^\top S_{i2}$. Substituting (38)–(41) into (36) yields

$$\begin{aligned} \dot{V}_{ilk} &\leq -\varrho_i(\underline{\lambda}(Q_{ik}) - 3r_{i0}e^{\beta\tau}) \|\varepsilon_i\|^2 + \omega_{il} \omega_{i,l+1} + \Theta_{ilk} \\ &\quad + \sum_{q=1}^l \left(\frac{\gamma_{iq}}{\ell_{iq}} \tilde{\theta}_{iq} \hat{\theta}_{iq} - c_{iq} \omega_{iq}^2 \right) - \bar{f}_{i0k}(X_0) \\ &\quad + \frac{\varrho_i e^{-\beta\tau}}{r_0} \|P_{ik}\|^2 \sum_{l=1}^m \sum_{j=1}^n (F_{ilj}^2(x_j) + H_{ilj}^2(x_{j\tau})) \\ &\quad + \frac{e^{-\beta\tau}}{2r_{i1}} \sum_{j=1}^n (F_{i1j}^2(x_j) + H_{i1j}^2(x_{j\tau})) \end{aligned} \quad (42)$$

where $c_{il} = \bar{c}_{il} - \frac{1}{2}$ and $\Theta_{ilk} = \Theta_{i,l-1,k} + \frac{e^{-\beta\tau}}{4r_{i1}} d_{il}^2 + \frac{1}{2} a_{il}^2 + \frac{1}{2} \delta_{il}^{*2}$.

Step m : Based on (8), (19), and (22), one also gets the following dynamics of ω_{im} as:

$$\dot{\omega}_{im} = u_{ik} + L_{imk} \varepsilon_{i1} - \dot{\alpha}_{im} - \dot{\xi}_{im}.$$

Let the Lyapunov function candidate be

$$V_{imk} = V_{i,m-1,k} + \frac{1}{2} \omega_{im}^2 + \frac{1}{2\ell_{im}} \tilde{\theta}_{im}^2 \quad (43)$$

where ℓ_{im} is a positive constant. Then, it is deduced that

$$\begin{aligned} \dot{V}_{imk} &= \omega_{il} [u_{ik} + L_{imk} \varepsilon_{i1} - \dot{\alpha}_{im} - \dot{\xi}_{im}] \\ &\quad + \dot{V}_{i,m-1,k} - \frac{1}{\ell_{im}} \tilde{\theta}_{im} \dot{\theta}_{im}. \end{aligned} \quad (44)$$

Utilizing Young's inequality induces

$$\omega_{im} d_{im} \text{sign}(\xi_{im}) \leq r_{im} e^{\beta\tau} \omega_{im}^2 + \frac{e^{-\beta\tau}}{4r_{im}} d_{im}^2 \quad (45)$$

where r_{im} is a positive parameter. To proceed, $\bar{f}_{imk}(X_{im}) = L_{imk} \varepsilon_{i1} - \dot{\alpha}_{im} + r_{im} e^{\beta\tau} \omega_{im}$ with $X_{im} = [x_{i1}, y_{ir}, y_{ir}^{(1)}, \dots, y_{ir}^{(m-1)}, \hat{\theta}_{i1}, \dots, \hat{\theta}_{i,m-1}, \hat{x}_{i1}, \dots, \hat{x}_{im}]^\top$.

Based on (3) and (4), a fuzzy logic system is given by

$$\bar{f}_{imk}(X_{il}) = W_{imk}^{*\top} S_{im} + \delta_{imk} \quad (46)$$

where δ_{imk} is the error of approximation and a positive constant δ_{im}^* is satisfied by $|\delta_{imk}| < \delta_{im}^*$. By using Young's inequality, Lemma 1, (12), and (46), one can obtain

$$\begin{aligned} \omega_{im} \bar{f}_{imk}(X_{im}) &= \omega_{im} W_{imk}^{*\top} S_{im} + \omega_{im} \delta_{imk} \\ &\leq \frac{1}{2a_{im}^2} \omega_{im}^2 \theta_{im}^* S_{im}^\top S_{im} + \frac{1}{2} a_{im}^2 + \frac{1}{2} \omega_{im}^2 + \frac{1}{2} \delta_{im}^{*2} \end{aligned} \quad (47)$$

where a_{im} is a positive parameter. Then, the actual controller input u_{ik} and the adaptive laws $\hat{\theta}_{im}$ can be determined as

$$u_{ik} = -\bar{c}_{imk} z_{im} - z_{i,m-1} - \frac{1}{2a_{im}^2} \omega_{im} \hat{\theta}_{im} S_{im}^\top S_{im} \quad (48)$$

$$\dot{\hat{\theta}}_{im} = \frac{\ell_{im}}{2a_{im}^2} \omega_{im}^2 S_{im}^\top S_{im} - \gamma_{im} \hat{\theta}_{im} \quad (49)$$

where γ_{im} is a positive constant. Combining (44)–(49) yields

$$\begin{aligned} \dot{V}_{imk} &\leq -\varrho_i(\underline{\lambda}(Q_{ik}) - 3r_{i0}e^{\beta\tau}) \|\varepsilon_i\|^2 + \Theta_{imk} - \bar{f}_{i0k}(X_0) \\ &\quad + \frac{\varrho_i e^{-\beta\tau}}{r_0} \|P_{ik}\|^2 \sum_{l=1}^m \sum_{j=1}^n (F_{ilj}^2(x_j) + H_{ilj}^2(x_{j\tau})) \\ &\quad + \frac{e^{-\beta\tau}}{2r_{i1}} \sum_{j=1}^n (F_{i1j}^2(x_j) + H_{i1j}^2(x_{j\tau})) \\ &\quad + \sum_{q=1}^m \left(\frac{\gamma_{iq}}{\ell_{iq}} \tilde{\theta}_{iq} \hat{\theta}_{iq} - c_{iq} \omega_{iq}^2 \right) \end{aligned} \quad (50)$$

where $c_{im} = \min_{k \in \mathbb{M}} \{\bar{c}_{imk} - \frac{1}{2}\}$ and $\Theta_{imk} = \Theta_{imk} + \frac{e^{-\beta\tau}}{4r_{im}} d_{im}^2 + \frac{1}{2} a_{im}^2 + \frac{1}{2} \delta_{im}^{*2}$.

C. Stability Analysis

First of all, for notational convenience, define

$$\mu_k = \min \left\{ \frac{\varrho_i(\underline{\lambda}(Q_{ik}) - 3r_{i0}e^{\beta\tau})}{\bar{\lambda}(P_{ik})}, 2c_{iq}, \gamma_{iq}, \beta, 2\bar{c}_{iq}, \right. \\ \left. i = 1, \dots, n, q = 1, \dots, m, k \in \mathbb{M} \right\} \quad (51)$$

$$v_k = \max \left\{ \frac{\bar{\lambda}(P_{ik})}{\underline{\lambda}(P_{ip})}, i = 1, \dots, n, k, p \in \mathbb{M} \right\} \quad (52)$$

where $\bar{\lambda}(P_{ik})$ ($\underline{\lambda}(P_{ik})$) refers to the largest (smallest) eigenvalue of the matrix P_{ik} , respectively. Obviously, the inequalities $\varrho_i(\underline{\lambda}(Q_{ik}) - 3r_{i0}e^{\beta\tau}) > 0, i = 1, \dots, n, q = 1, \dots, m, k \in \mathbb{M}$ holds by suitably selecting $Q_{ik}, \varrho_i, r_{i0}$ and β . Then, $\mu_k > 0$ and $v_k \geq 1$ are the two designed parameters.

Theorem 1: Consider the switched nonlinear MIMO-delayed system (1) satisfying Assumptions 1 and 2. The adaptive fuzzy output feedback funnel controllers (48) with the switched state observer (8), the switched command filter (20), the virtual controllers (32), (40), and the adaptive laws (33), (41), (49) can ensure all the closed-loop signals achieve semiglobally uniformly ultimate bounded; then the tracking errors $y_i - y_{ir}$ for $i = 1, \dots, n$ converge to the prespecified performance funnels under a category of switching signals with MDADT. The block diagram of the proposed control scheme is depicted in Fig. 3.

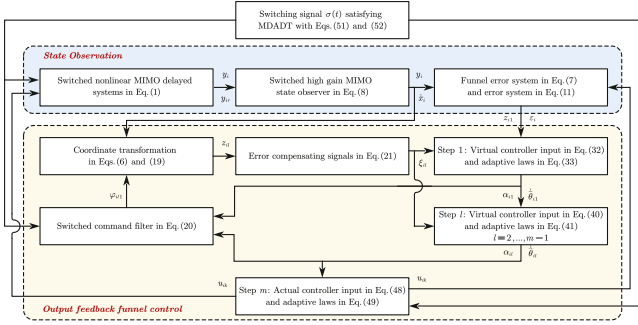


Fig. 3. Block diagram of the proposed control scheme.

Proof: The proof consists of two parts to analyze the boundedness of all signals in the closed-loop system. In part 1), the semiglobal stability is verified for the switched system with a category of switching signals satisfying MDADT. In part 2), the output tracking errors are verified to converge to the prespecified performance funnels.

1) To analyze the stability of the compensating signal (21), let the Lyapunov function candidate be

$$V_{i\xi} = \frac{1}{2} \sum_{q=1}^m \xi_{iq}^2 \quad (53)$$

and calculate its time derivative. Then, one has

$$\dot{V}_{i\xi} = - \sum_{q=1}^m \bar{c}_{iq} \xi_{iq}^2 + \sum_{q=1}^{m-1} \Gamma_{iq} \left[(\bar{\alpha}_{i,q+1} - \alpha_{iq}) \xi_{iq} - d_{iq} |\xi_{iq}| \right] \quad (54)$$

where $\bar{c}_{im} = \min_{k \in M} \{\bar{c}_{imk}\}$ and $\Gamma_{iq} = 1$ for $q = 2, \dots, m-1$. Similar to those in [35], $|\bar{\alpha}_{i,q+1} - \alpha_{iq}| \leq \alpha_{iq}^*$ can be approached in a finite time with known constants α_{iq}^* for $i = 1, \dots, n$ and $q = 2, \dots, m-1$. To proceed, by selecting appropriate parameters $d_{iq} \geq \alpha_{iq}^*$, it yields

$$\begin{aligned} \dot{V}_{i\xi} &\leq - \sum_{q=1}^m \bar{c}_{iq} \xi_{iq}^2 + \sum_{q=1}^{m-1} \Gamma_{iq} \left(\alpha_{iq}^* |\xi_{iq}| - d_{iq} |\xi_{iq}| \right) \\ &\leq - \sum_{q=1}^m \bar{c}_{iq} \xi_{iq}^2. \end{aligned} \quad (55)$$

Here, based on (13), (24), (35), (43), and (53), the following multiple Lyapunov–Krasovskii functions are constructed by

$$V_k(X) = \sum_{i=1}^n (V_{imk}(X_i) + V_{iLK} + V_{i\xi}), \quad k \in \mathbb{M} \quad (56)$$

where $X = [X_1^\top, \dots, X_n^\top]^\top$, $X_i = [\varepsilon_i^\top, \omega_{i1}, \dots, \omega_{im}, \bar{\theta}_{i1}, \dots, \bar{\theta}_{im}, \xi_{i1}, \dots, \xi_{im}]^\top$, and $V_{iLK} = \frac{e^{-\beta t}}{1-\bar{\tau}} \sum_{j=1}^n \int_{t-\tau_j(t)}^t e^{\beta s} \nu_j(x_j(s)) ds$ with $\nu_j(x_j) = \frac{\varrho_i}{r_0} \|P_{ik}\|^2 \sum_{l=1}^m H_{ilj}^2(x_j) + \frac{1}{2r_{i1}} H_{i1j}^2(x_j)$. In addition, it induces

$$\dot{V}_k \leq \sum_{i=1}^n \left[-\varrho_i (\underline{\lambda}(Q_{ik}) - 3r_{i0} e^{\beta\tau}) \|\varepsilon_i\|^2 + \Theta_{imk} - \bar{f}_{i0k}(X_0) \right.$$

$$\begin{aligned} &+ \frac{\varrho_i e^{-\beta\tau}}{r_0} \|P_{ik}\|^2 \sum_{l=1}^m \sum_{j=1}^n F_{ilj}^2(x_j) - \beta V_{iLK} \\ &+ \frac{e^{-\beta\tau}}{2r_{i1}} \sum_{j=1}^n F_{i1j}^2(x_j) + \sum_{q=1}^m \left(\frac{\gamma_{iq}}{\ell_{iq}} \bar{\theta}_{iq} \hat{\theta}_{iq} - c_{iq} \omega_{iq}^2 \right) \\ &+ \sum_{j=1}^n \frac{1}{1-\bar{\tau}} \nu_j(x_j) - \sum_{q=1}^m \bar{c}_{iq} \xi_{iq}^2 \Big]. \end{aligned} \quad (57)$$

To proceed, denote the function $\bar{f}_{i0k}(X_0)$, $k \in \mathbb{M}$ as

$$\begin{aligned} \bar{f}_{i0k}(X_0) &= \frac{\varrho_i e^{-\beta\tau}}{r_0} \|P_{ik}\|^2 \sum_{l=1}^m F_{ilj}^2(x_j) + \frac{e^{-\beta\tau}}{2r_{i1}} F_{i1j}^2(x_j) \\ &+ \frac{1}{1-\bar{\tau}} \nu_j(x_j). \end{aligned} \quad (58)$$

Furthermore, the term $\frac{\gamma_{iq}}{\ell_{iq}} \bar{\theta}_{iq} \hat{\theta}_{iq}$ from (57) satisfies

$$\frac{\varrho_{iq}}{\ell_{iq}} \bar{\theta}_{iq} \hat{\theta}_{iq} \leq \frac{\varrho_{iq}}{2\ell_{iq}} \theta_{iq}^{*2} - \frac{\varrho_{iq}}{2\ell_{iq}} \bar{\theta}_{iq}^2 \quad (59)$$

where $\hat{\theta}_{iq} = \theta_{iq}^* - \bar{\theta}_{iq}$. According to (57)–(59), one has

$$\begin{aligned} \dot{V}_k &\leq \sum_{i=1}^n \left[-\varrho_i (\underline{\lambda}(Q_{ik}) - 3r_{i0} e^{\beta\tau}) \|\varepsilon_i\|^2 - \beta V_{iLK} + \Theta_i \right. \\ &\quad \left. - \sum_{q=1}^m \left(\frac{\gamma_{iq}}{2\ell_{iq}} \bar{\theta}_{iq}^2 + c_{iq} \omega_{iq}^2 + \bar{c}_{iq} \xi_{iq}^2 \right) \right] \\ &\leq -\mu_k V_k + \Theta \end{aligned} \quad (60)$$

where $\Theta = \sum_{i=1}^n \Theta_i = \sum_{i=1}^n (\Theta_{imk} + \sum_{q=1}^m \frac{\varrho_{iq}}{2\ell_{iq}} \theta_{iq}^{*2})$. It is clear that if the function $\underline{\kappa}(\cdot) \in \mathcal{K}_\infty$ exists, the following inequality holds:

$$\begin{aligned} V_k(X) &\geq \sum_{i=1}^n \left[\varrho_i \varepsilon_i^\top P_{ik} \varepsilon_i + \sum_{q=1}^m \left(\frac{1}{2} \omega_{iq}^2 + \frac{1}{2\ell_{iq}} \bar{\theta}_{iq}^2 + \frac{1}{2} \xi_{iq}^2 \right) \right] \\ &\geq \underline{\kappa}(\|X\|). \end{aligned} \quad (61)$$

Moreover, it can be verified from (56) that

$$\begin{aligned} V_{iLK} &\leq \frac{e^{-\beta t}}{1-\bar{\tau}} \sum_{j=1}^n \int_{-\tau_j(t)}^0 e^{\beta(t+s)} \nu_j(x_j(t+s)) d(t+s) \\ &\leq \frac{e^{-\beta t}}{1-\bar{\tau}} \sum_{j=1}^n \sup_{-\tau_j(t) \leq s < 0} \tau_j(t) e^{\beta(t+s)} \nu_j(x_j(t+s)). \end{aligned} \quad (62)$$

Meanwhile, concerned with a function $\bar{\kappa}(\cdot) \in \mathcal{K}_\infty$, one gets

$$\begin{aligned} V_k(X) &\leq \sup_{-\tau_j(t) \leq s \leq 0} \sum_{i=1}^n \left[\varrho_i \varepsilon_i(t+s)^\top P_{ik} \varepsilon_i(t+s) + \right. \\ &\quad \left. \sum_{q=1}^m \left(\frac{1}{2} \omega_{iq}^2(t+s) + \frac{1}{2\ell_{iq}} \bar{\theta}_{iq}^2(t+s) + \frac{1}{2} \xi_{iq}^2(t+s) \right) \right] \\ &\leq \bar{\kappa} \left(\sup_{-\tau \leq s \leq 0} \|X(t+s)\| \right). \end{aligned} \quad (63)$$

Thus, based on (61) and (63), two functions $\underline{\kappa}(\cdot), \bar{\kappa}(\cdot) \in \mathcal{K}_\infty$ satisfy

$$\underline{\kappa}(\|X\|) \leq V_k(X) \leq \bar{\kappa}\left(\sup_{-\tau \leq s \leq 0} \|X(t+s)\|\right). \quad (64)$$

According to the definition (52), one can obtain

$$V_k(X) \leq v_k V_p(X) \quad \forall k, p \in M. \quad (65)$$

Let the initial time be $t_0 = 0$. Let the each switching time be $t_1, \dots, t_j, t_{j+1}, \dots, t_{N_\sigma(T,0)}$ on the instant $[0, T]$ with $N_\sigma(T, 0) = \sum_{k=1}^{\bar{M}} N_{\sigma k}(T, 0)$, $k \in \mathbb{M}$. Consider the following function:

$$\Phi(t) = e^{\mu_{\sigma(t)} t} V_{\sigma(t)}(X(t)). \quad (66)$$

Based on (60) and (66), one gets $\dot{\Phi}(t) \leq \Theta e^{\mu_{\sigma(t)} t}$. On some instant $[t_j, t_{j+1})$, it implies from (65) that

$$\begin{aligned} \Phi(t_{j+1}) &= e^{\mu_{\sigma(t_{j+1})} t_{j+1}} V_{\sigma(t_{j+1})}(X(t_{j+1})) \\ &\leq v_{\sigma(t_{j+1})} e^{\mu_{\sigma(t_{j+1})} t_{j+1}} V_{\sigma(t_j)}(X(t_{j+1})) \\ &= v_{\sigma(t_{j+1})} e^{(\mu_{\sigma(t_{j+1})} - \mu_{\sigma(t_j)}) t_{j+1}} \Phi(t_{j+1}^-) \\ &\leq v_{\sigma(t_{j+1})} e^{(\mu_{\sigma(t_{j+1})} - \mu_{\sigma(t_j)}) t_{j+1}} \left(\Phi(t_j) + \int_{t_j}^{t_{j+1}} \Theta e^{\mu_{\sigma(t_j)} t} dt \right) \\ &\leq v_{\sigma(t_{j+1})} e^{(\mu_{\sigma(t_{j+1})} - \mu_{\sigma(t_j)}) t_{j+1}} \left[v_{\sigma(t_j)} e^{(\mu_{\sigma(t_j)} - \mu_{\sigma(t_{j-1})}) t_j} \right. \\ &\quad \times \left(\Phi(t_{j-1}) + \int_{t_{j-1}}^{t_j} \Theta e^{\mu_{\sigma(t_{j-1})} t} dt \right) + \left. \int_{t_j}^{t_{j+1}} \Theta e^{\mu_{\sigma(t_j)} t} dt \right] \\ &\leq \prod_{l=0}^j v_{\sigma(t_{l+1})} e^{\sum_{l=0}^j (\mu_{\sigma(t_{l+1})} - \mu_{\sigma(t_l)}) t_{l+1}} \Phi(t_0) \\ &\quad + \sum_{s=0}^j \left(\prod_{l=s}^j v_{\sigma(t_{l+1})} e^{\sum_{l=s}^j (\mu_{\sigma(t_{l+1})} - \mu_{\sigma(t_l)}) t_{l+1}} \right. \\ &\quad \times \left. \int_{t_s}^{t_{s+1}} \Theta e^{\mu_{\sigma(t_s)} t} dt \right). \end{aligned} \quad (67)$$

On the instant $[0, T]$, iterating the inequality (67) from $l = 0$ to $l = N_\sigma(T, 0) - 1$, it induces

$$\begin{aligned} \Phi(T^-) &\leq \Phi(t_{N_\sigma(T,0)}) + \int_{t_{N_\sigma(T,0)}}^T \Theta e^{\mu_{\sigma(t)} t} dt \\ &\leq \prod_{l=0}^{N_\sigma(T,0)-1} v_{\sigma(t_{l+1})} e^{\sum_{l=0}^{N_\sigma(T,0)-1} (\mu_{\sigma(t_{l+1})} - \mu_{\sigma(t_l)}) t_{l+1}} \Phi(t_0) \\ &\quad + \sum_{s=0}^{N_\sigma(T,0)-1} \left[\prod_{l=s}^{N_\sigma(T,0)-1} v_{\sigma(t_{l+1})} \int_{t_s}^{t_{s+1}} \Theta e^{\mu_{\sigma(t_s)} t} dt \right. \\ &\quad \times \left. e^{\sum_{l=s}^{N_\sigma(T,0)-1} (\mu_{\sigma(t_{l+1})} - \mu_{\sigma(t_l)}) t_{l+1}} \right] \\ &\quad + \int_{t_{N_\sigma(T,0)}}^T \Theta e^{\mu_{\sigma(t)} t} dt. \end{aligned} \quad (68)$$

Based on (66) and (68), one has

$$\begin{aligned} V_{\sigma(T^-)}(X(T)) &\leq \prod_{k=1}^{\bar{M}} v_k^{N_{\sigma k}(T,0)} V_{\sigma(0)}(X(0)) \\ &\quad \times e^{-\sum_{k=1}^{\bar{M}} [\mu_k \sum_{s \in \Psi(k)} (t_{s+1} - t_s)] - \mu_{\sigma(t_{N_\sigma(T,0)})} (T - t_{N_\sigma(T,0)})} \\ &\quad + \sum_{s=0}^{N_\sigma(T,0)-1} \left[\prod_{l=s}^{N_\sigma(T,0)-1} v_{\sigma(t_{l+1})} \right. \\ &\quad \times \left. e^{\sum_{l=s}^{N_\sigma(T,0)-1} (\mu_{\sigma(t_{l+1})} - \mu_{\sigma(t_l)}) t_{l+1} - \mu_{\sigma(t_{N_\sigma(T,0)})} T + \mu_{\sigma(t_s)} t_{s+1}} \right. \\ &\quad \times \left. e^{-\eta_{\min} t_{s+1}} \int_{t_s}^{t_{s+1}} \Theta e^{\eta_{\min} t} dt \right] \\ &\quad + e^{-\eta_{\min} T} \int_{t_{N_\sigma(T,0)}}^T \Theta e^{\eta_{\min} t} dt \\ &\leq e^{\sum_{k=1}^{\bar{M}} N_{0k} \ln v_k} e^{\sum_{k=1}^{\bar{M}} \frac{T_k}{\tau_{ak}} \ln v_k - \sum_{k=1}^{\bar{M}} \mu_k T_k} V_{\sigma(0)}(X(0)) \\ &\quad + \sum_{s=0}^{N_\sigma(T,0)-1} \left[\prod_{k=1}^{\bar{M}} v_k^{N_{\sigma k}(T, t_{s+1})} e^{-\sum_{k=1}^{\bar{M}} \mu_k T_k(T, t_{s+1})} \right. \\ &\quad \times \left. e^{-\eta_{\min} t_{s+1}} \int_{t_s}^{t_{s+1}} \Theta e^{\eta_{\min} t} dt \right] \\ &\quad + e^{-\eta_{\min} T} \int_{t_{N_\sigma(T,0)}}^T \Theta e^{\eta_{\min} t} dt \end{aligned} \quad (69)$$

where $\Psi(k)$ is the set of s satisfying $\sigma(t_s) = k$ with $t_s \in \{t_0, t_1, \dots, t_j, t_{j+1}, \dots, t_{N_\sigma(T,0)-1}\}$ and $\eta_{\min} = \min\{\eta_k, k \in \mathbb{M}\}$ with $\eta_k \in (0, \mu_k - \frac{\ln v_k}{\tau_{ak}})$. By utilizing $\tau_{ak} \geq \frac{\ln v_k}{\mu_k}$, for any $\eta_k \in (0, \mu_k - \frac{\ln v_k}{\tau_{ak}})$, one obtains $\tau_{ak} \geq \frac{\ln v_k}{\mu_k - \eta_k}$. Based on Definition 1, it yields $N_{\sigma k}(T, t) \leq N_{0k} + \frac{(\mu_k - \eta_k) T_k(T, t)}{\ln v_k}$, which implies that

$$v_k^{N_{\sigma k}(T, t_{s+1})} \leq v_k^{N_{0k}} e^{(\mu_k - \eta_k) T_k(T, t_{s+1})}. \quad (70)$$

Together with (69) and (70), one gets

$$\begin{aligned} V_{\sigma(T^-)}(X(T)) &\leq e^{\sum_{k=1}^{\bar{M}} N_{0k} \ln v_k} e^{\sum_{k=1}^{\bar{M}} \left(\frac{\ln v_k}{\tau_{ak}} - \mu_k \right) T_k} V_{\sigma(0)}(X(0)) \\ &\quad + \sum_{s=0}^{N_\sigma(T,0)-1} \left[\prod_{k=1}^{\bar{M}} v_k^{N_{0k}} e^{-\eta_{\min} (T - t_{s+1})} \right. \\ &\quad \times \left. e^{-\eta_{\min} t_{s+1}} \int_{t_s}^{t_{s+1}} \Theta e^{\eta_{\min} t} dt \right] \\ &\quad + e^{-\eta_{\min} T} \int_{t_{N_\sigma(T,0)}}^T \Theta e^{\eta_{\min} t} dt \\ &\leq e^{\sum_{k=1}^{\bar{M}} N_{0k} \ln v_k} e^{\sum_{k=1}^{\bar{M}} \left(\frac{\ln v_k}{\tau_{ak}} - \mu_k \right) T_k} V_{\sigma(0)}(X(0)) \end{aligned}$$

$$\begin{aligned}
& + \prod_{k=1}^{\bar{M}} v_k^{N_{0k}} e^{-\eta_{\min} T} \int_0^T \Theta e^{\eta_{\min} t} dt \\
& \leq e^{\sum_{k=1}^{\bar{M}} N_{0k} \ln v_k} e^{\max_{k \in \mathbb{M}} \left(\frac{\ln v_k}{\tau_{ak}} - \mu_k \right) T} V_{\sigma(0)}(X(0)) \\
& + \prod_{k=1}^{\bar{M}} v_k^{N_{0k}} \frac{\Theta}{\eta_{\min}} \quad (71)
\end{aligned}$$

which implies for any $T > 0$ that

$$\begin{aligned}
\kappa(\|X(T)\|) & \leq e^{\sum_{k=1}^{\bar{M}} N_{0k} \ln v_k} e^{\max_{k \in \mathbb{M}} \left(\frac{\ln v_k}{\tau_{ak}} - \mu_k \right) T} \\
& \times \bar{\kappa} \left(\sup_{-\tau \leq s \leq 0} \|X(s)\| \right) + \prod_{k=1}^{\bar{M}} v_k^{N_{0k}} \frac{\Theta}{\eta_{\min}}. \quad (72)
\end{aligned}$$

Therefore, it can be concluded by (71) that if the MDADT satisfies $\tau_{ak} \geq \frac{\ln v_k}{\mu_k}$ for $k \in \mathbb{M}$, ε_{il} , ω_{il} , θ_{il} , and ξ_{il} for $i = 1, \dots, n$ and $l = 1, \dots, m$ are bounded for any bounded initial values. According to the definition of θ_{il} for $i = 1, \dots, n$ and $l = 1, \dots, m$, one can know that $\hat{\theta}_{il}$ are bounded. Based on (22), z_{il} for $i = 1, \dots, n$ and $l = 1, \dots, m$ are bounded. Then, through (32), (40), and (48), one gets α_{il} and u_{ik} for $i = 1, \dots, n$, $l = 1, \dots, m-1$, and $k \in \mathbb{M}$ are bounded. Next, based on the switched command filter (20), signals $\bar{\alpha}_{il}$ and $\dot{\bar{\alpha}}_{il}$ for $i = 1, \dots, n$ and $l = 2, \dots, m$ are bounded. Based on (19), \hat{x}_{il} for $i = 1, \dots, n$ and $l = 2, \dots, m$ are bounded. According to (5), (6), (10), it yields that x_{il} for $i = 1, \dots, n$ and $l = 1, \dots, m$ are also bounded. Hence, for $k \in \mathbb{M}$, all the signals in the closed-loop system are bounded under a category of switching signals with MDADT satisfying $\tau_{ak} \geq \frac{\ln v_k}{\mu_k}$.

2) In what follows, based on (56) and (72), one has

$$\begin{aligned}
\frac{1}{2} \omega_{i1}^2(T) & \leq e^{\sum_{k=1}^{\bar{M}} N_{0k} \ln v_k} e^{\max_{k \in \mathbb{M}} \left(\frac{\ln v_k}{\tau_{ak}} - \mu_k \right) T} \\
& \times \bar{\kappa} \left(\sup_{-\tau \leq s \leq 0} \|X(s)\| \right) + \prod_{k=1}^{\bar{M}} v_k^{N_{0k}} \frac{\Theta}{\eta_{\min}}. \quad (73)
\end{aligned}$$

Then, together with $\tau_{ak} \geq \frac{\ln v_k}{\mu_k}$ and the definitions in (6), (22), and (73), one has

$$\begin{aligned}
\frac{\varepsilon_{iy}^2(T)}{F_{i\psi}^2(T) - \varepsilon_{iy}^2(T)} & \leq 4 \left(e^{\sum_{k=1}^{\bar{M}} N_{0k} \ln v_k} \bar{\kappa} \left(\sup_{-\tau \leq s \leq 0} \|X(s)\| \right) \right. \\
& \left. + \prod_{k=1}^{\bar{M}} v_k^{N_{0k}} \frac{\Theta}{\eta_{\min}} \right) + 2\|\xi_{i1}(T)\|^2. \quad (74)
\end{aligned}$$

According to (53) and (55), one gets

$$V_{i\xi}(t) = \frac{1}{2} \sum_{q=1}^m \xi_{iq}^2 \leq V_{i\xi}(0) e^{-\bar{c}_i t} \quad (75)$$

where $\bar{c}_i = 2 \min\{\bar{c}_{iq}, q = 1, \dots, m\}$. Based on (5), (74), and (75), it yields

$$\lim_{t \rightarrow \infty} \varepsilon_{i1}^2(t) = \lim_{t \rightarrow \infty} |y_i(t) - y_{ir}(t)|^2 \leq \epsilon_i^2$$

where $\epsilon_i^2 = [4(e^{\sum_{k=1}^{\bar{M}} N_{0k} \ln v_k} \bar{\kappa}(\sup_{-\tau \leq s \leq 0} \|X(s)\|) + \prod_{k=1}^{\bar{M}} v_k^{N_{0k}} \frac{\Theta}{\eta_{\min}})] / [1 + 4(e^{\sum_{k=1}^{\bar{M}} N_{0k} \ln v_k} \bar{\kappa}(\sup_{-\tau \leq s \leq 0} \|X(s)\|) + \prod_{k=1}^{\bar{M}} v_k^{N_{0k}} \frac{\Theta}{\eta_{\min}})]$.

$\|X(s)\| + \prod_{k=1}^{\bar{M}} v_k^{N_{0k}} \frac{\Theta}{\eta_{\min}}]$. Thus, the tracking errors $y_i(t) - y_{ir}(t)$ for $i = 1, \dots, n$ can stay within the prespecified performance funnels by suitably selecting Q_{ik} , ϱ_i , r_{i0} , β , and d_{il} for $i = 1, \dots, n$, $l = 1, \dots, m$, and $k \in \mathbb{M}$. The proof has been completed. ■

Remark 3: A detailed guideline from Step 1) to Step 5) is provided to elucidate the design of parameters for the proposed output-feedback funnel control strategy as follows.

- 1) Set initial conditions and funnel boundary parameters ρ_{it_0} , ρ_{iT_f} , T_f satisfying $\|\varepsilon_{iy}(t_0)\| < F_{i\psi}(t_0)$.
- 2) Select the proper parameters L_{ilk} , such that the matrices A_{ik} are Hurwitz for $i = 1, \dots, n$, $l = 1, \dots, m$ and $k \in \mathbb{M}$. Then, after specifying the symmetric matrices $Q_{ik} > 0$, the symmetric matrices $P_{ik} > 0$ can be calculated by solving (9).
- 3) Decide the number of fuzzy IF-THEN rules and fuzzy basic functions, then determine the fuzzy logic systems (3).
- 4) Select suitable controller design parameters ϖ_{ik} , ζ_{ik} , \bar{c}_{il} , \bar{c}_{imk} , d_{il} , ℓ_{il} , a_{il} , and γ_{il} for $i = 1, \dots, n$, $l = 1, \dots, m$ and $k \in \mathbb{M}$, and then determine the controllers (32), (40), and (48) with the adaptive laws (33), (41), and (49).
- 5) Determine the designed parameters of MDADT with $\mu_k > 0$ in (51) and $v_k \geq 1$ in (52).

Remark 4: Although backstepping control, dynamic surface control, and funnel control all aim to stabilize nonlinear systems and achieve desired tracking performance, they differ significantly in their methodologies and performance guarantees. Backstepping control and dynamic surface control focus on a recursive design with dynamic surface control mitigating complexity issues in [9], [15], and [36], whereas funnel control emphasizes maintaining the error within a predefined boundary, offering a unique approach to guarantee performance.

Remark 5: It is worth pointing out that, for non-switched nonlinear systems, some adaptive control strategies have been developed in [16], [21], and [22] via backstepping control or dynamic surface control. However, these existing adaptive control schemes for nonswitched nonlinear systems cannot be directly applied to improve the requirements in the transient and the steady-state performance of switched nonlinear MIMO-delayed systems within the complexity caused by time delays and subsystem switching. Hence, to overcome this conservativeness, this article has proposed the funnel control method for switched nonlinear MIMO-delayed systems. Meanwhile, the funnel control method offers robust transient performance by quickly reducing the error within a shrinking boundary [24], [25]. It ensures stable and predictable steady-state performance by confining the error within a predefined small bound.

IV. CASE STUDIES

This section provides two case studies to show the effectiveness and flexibility of the proposed fuzzy output-feedback funnel control strategy on the switched nonlinear MIMO-delayed systems.

Example 1: Two inverted pendulums over the controller area network with time-varying delays in the transmission of their

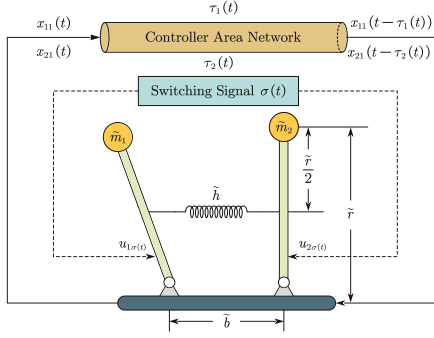


Fig. 4. Schematic of two inverted pendulums over the controller area network.

measurements are considered via the switching control. Based on [37] and [38], the dynamics of the two inverted pendulums is defined as

$$\dot{x}_{11} = x_{12} \quad (76a)$$

$$\begin{aligned} \dot{x}_{12} = & \left(\frac{\tilde{m}_1 g \tilde{r}}{J_1} - \frac{\tilde{h} \tilde{r}^2}{4J_1} \right) \sin(x_{11}(t - \tau_1(t))) + \frac{\tilde{h} \tilde{r}}{2J_1} (\bar{l} - \tilde{b}) \\ & + \frac{u_{1\sigma(t)}}{J_1} + \frac{\tilde{h} \tilde{r}^2}{4J_1} \sin(x_{21}(t - \tau_2(t))) \end{aligned} \quad (76b)$$

$$\dot{x}_{21} = x_{22} \quad (76c)$$

$$\begin{aligned} \dot{x}_{22} = & \left(\frac{\tilde{m}_2 g \tilde{r}}{J_2} - \frac{\tilde{h} \tilde{r}^2}{4J_2} \right) \sin(x_{21}(t - \tau_2(t))) - \frac{\tilde{h} \tilde{r}}{2J_2} (\bar{l} - \tilde{b}) \\ & + \frac{u_{2\sigma(t)}}{J_2} + \frac{\tilde{h} \tilde{r}^2}{4J_2} \sin(x_{12}) \end{aligned} \quad (76d)$$

where $\sigma(t) \rightarrow \{1, 2\}$, x_{11} and x_{21} are the angular displacements of the left and right pendulum from vertical, respectively, x_{12} and x_{22} stand for the angular rates of the left and right pendulum from vertical, respectively, \tilde{m}_1 and \tilde{m}_2 represent the pendulum end masses, J_1 and J_2 stand for the moments of inertia, g is the gravity coefficient, \tilde{r} represents the pendulum height, \tilde{h} is the spring constant of the connecting spring, \bar{l} stands for the natural length of the spring, and \tilde{b} represents the distance between the pendulum hinges (see Fig. 4 for details). Then, the switched MIMO high-gain state observer is constructed as

$$\dot{\hat{x}}_{i1} = \hat{x}_{i2} + L_{i1\sigma(t)}(y_i - \hat{x}_{i1}) \quad (77a)$$

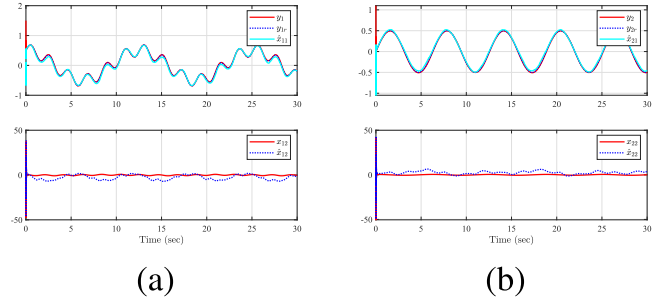
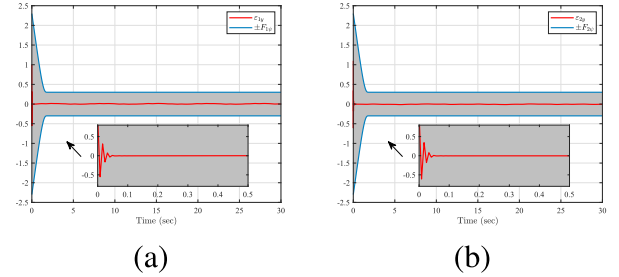
$$\dot{\hat{x}}_{i2} = u_{i\sigma(t)} + L_{i2\sigma(t)}(y_i - \hat{x}_{i1}) \quad (77b)$$

and the parameters are chosen as $L_{i11} = 100$, $L_{i21} = 100$, $L_{i12} = 80$, and $L_{i22} = 80$ such that A_{i1} and A_{i2} are Hurwitz matrices. To proceed, one selects $Q_{i1} = 6I_2$ and $Q_{i2} = 5I_2$ with $I_2 = \text{diag}\{1, 1\}$. Meanwhile, the symmetric positive definite matrices are

$$P_{i1} = \begin{bmatrix} 3.03 & -3.00 \\ -3.00 & 3.03 \end{bmatrix}, P_{i2} = \begin{bmatrix} 2.53 & -2.50 \\ -2.50 & 2.53 \end{bmatrix}$$

satisfying (9). Then, the relevant control information is designed as

$$\alpha_{i1} = -\Gamma_{i1}^{-1} \left[\bar{c}_{i1} z_{i1} + \frac{1}{2a_{i1}^2} \omega_{i1} \hat{\theta}_{i1} S_{i1}^\top S_{i1} \right] \quad (78)$$

Fig. 5. (a) System output y_1 , reference signal y_{1r} , system state x_{12} , and estimated states \hat{x}_{11} and \hat{x}_{12} . (b) System output y_2 , reference signal y_{2r} , system state x_{22} , and estimated states \hat{x}_{21} and \hat{x}_{22} (Example 1).Fig. 6. Output tracking error. (a) ε_{1y} and (b) ε_{2y} in the prespecified performance funnel (Example 1).

$$\dot{\hat{\theta}}_{il} = \frac{\ell_{il}}{2a_{il}^2} \omega_{il}^2 S_{il}^\top S_{il} - \gamma_{il} \hat{\theta}_{il}, \quad i = 1, 2 \quad (79)$$

$$u_{ik} = -\bar{c}_{i2k} z_{i2} - z_{i,1} - \frac{1}{2a_{i2}^2} \omega_{i2} \hat{\theta}_{i2} S_{i2}^\top S_{i2}. \quad (80)$$

In Example 1, the parameters from the system (76) are selected as $\tilde{m}_1 = 2 \text{ kg}$, $\tilde{m}_2 = 2.5 \text{ kg}$, $J_1 = J_2 = 1 \text{ kg}$, $g = 9.8 \text{ m/s}^2$, $\tilde{r} = 0.5 \text{ m}$, $\tilde{h} = 100 \text{ N/m}$, $\bar{l} = 0.5 \text{ kg}$, $\tau_1(t) = \tau_2(t) = 0.01(1 + \sin(t)^2)$, and $\tilde{b} = 0.4 \text{ m}$. The design parameters are taken as $c_{i1} = 500$, $c_{i21} = 500$, $c_{i22} = 480$, $a_{il} = 10$, $\ell_{il} = 50$, $\gamma_{il} = 10$, $\zeta_{i1} = 0.9$, $\zeta_{i2} = 1$, $\varpi_{i1} = 1300$, $\varpi_{i2} = 1500$, $d_{il} = 0.1$, $\varrho_i = 20$, $\beta = 20$, and $r_{i0} = 2$ for $i = 1, 2$ and $l = 1, 2$. Then, it can be obtained by (51) and (52) that $\mu_1 = 10.01$, $v_1 = 200$, $\mu_2 = 8.02$, and $v_2 = 160$. The parameters of funnels are chosen as $\rho_{it0} = 2$, $\rho_{iTf} = 0.3$, and $T_f = 2$ for $i = 1, 2$. Based on Theorem 1, it can be concluded that all the signals in the closed-loop system are bounded under a category of switching signals with MDADT satisfying $\tau_{a1} = 0.53 \geq \frac{\ln v_1}{\mu_1}$ and $\tau_{a2} = 0.64 \geq \frac{\ln v_2}{\mu_2}$.

The initial vectors are provided as $[x_{11}(t_0), x_{12}(t_0), x_{21}(t_0), x_{22}(t_0)]^\top = [1.5, 0.2, 1.1, 0.1]^\top$, $[\hat{x}_{11}(t_0), \hat{x}_{12}(t_0), \hat{x}_{21}(t_0), \hat{x}_{22}(t_0)]^\top = [0.1, 0.2, 0.1, 0.4]^\top$, $\hat{\theta}_{11}(t_0) = 5$, $\hat{\theta}_{12}(t_0) = 3$, $\hat{\theta}_{21}(t_0) = 2$, $\hat{\theta}_{22}(t_0) = 5$, $\xi_{i1}(t_0) = 0$, $\xi_{i2}(t_0) = 0$, $\varphi_{i11}(t_0) = 0$, and $\varphi_{i12}(t_0) = 0$ for $t_0 \in [-0.02, 0]$. The reference signals are $y_{1r} = 0.2 \sin(3t) + 0.5 \cos(0.5t)$ and $y_{2r} = 0.5 \sin(t)$. Simulation results are described in Figs. 5–7. It is clear that, observed from the figures, all the signals in the closed-loop switched system are bounded. Besides, the output tracking errors $y_i - y_{ir}$ ($i = 1, 2$) converge to the pre-specified performance funnels with MDADT.

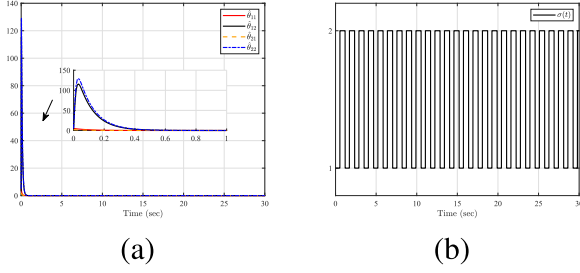


Fig. 7. (a) Adaptive laws $\hat{\theta}_{11}$, $\hat{\theta}_{12}$, $\hat{\theta}_{21}$, and $\hat{\theta}_{22}$. (b) Switching signal $\sigma(t)$ (Example 1).

Example 2: The switched nonlinear MIMO-delayed systems is considered as

$$\dot{x}_{i1} = x_{i2} + f_{i1\sigma(t)}(x) + h_{i1\sigma(t)}(x_\tau) \quad (81a)$$

$$\dot{x}_{i2} = u_{i\sigma(t)} + f_{i2\sigma(t)}(x) + h_{i2\sigma(t)}(x_\tau) \quad (81b)$$

where $i = 1, 2, \sigma(t) \rightarrow \{1, 2\}$, $f_{111} = x_{11} \sin(x_{21}x_{12})$, $h_{111} = 0.1 \sin(x_{11\tau}x_{22\tau})$, $f_{121} = x_{11}e^{0.1 \sin(x_{11})}$, $h_{121} = x_{12} \sin(x_{21}x_{12\tau}^2)$, $f_{211} = 0.1 \sin(x_{21}x_{12} - 0.2)$, $h_{211} = x_{21} \sin(x_{21\tau}x_{12})$, $f_{221} = x_{21}e^{0.2 \sin(x_{21})}$, $h_{221} = x_{21} \sin(x_{11\tau}x_{22\tau}^2)$, $f_{112} = 0.9x_{11} \sin(x_{21}x_{12})$, $h_{112} = 0.5 \sin(x_{11\tau}x_{22\tau})$, $f_{122} = x_{11}e^{0.1 \sin(x_{11})}$, $h_{122} = x_{12} \cos(x_{21}x_{12\tau}^2)$, $f_{212} = 0.1 \sin(x_{21}x_{12} - 0.2)$, $h_{212} = x_{21} \sin(x_{21\tau}x_{12})$, $f_{222} = 1.1x_{21}e^{0.2 \cos(x_{21})}$, $h_{222} = x_{21} \cos(x_{11\tau}x_{22\tau}^2)$, and $\tau_1(t) = \tau_2(t) = 0.1(1 + \cos(t)^2)$. Then, the switched MIMO high-gain state observer is the same as Example 1 in (77). To proceed, the parameters are chosen as $L_{i11} = 10$, $L_{i21} = 10$, $L_{i12} = 15$, and $L_{i22} = 15$ such that A_{i1} and A_{i2} are Hurwitz matrices. To proceed, one selects $Q_{i1} = 15I_2$ and $Q_{i2} = 10I_2$ with $I_2 = \text{diag}\{1, 1\}$. Meanwhile, the symmetric positive definite matrices are

$$P_{i1} = \begin{bmatrix} 8.25 & -7.50 \\ -7.50 & 8.33 \end{bmatrix}, P_{i2} = \begin{bmatrix} 5.34 & -5.00 \\ -5.00 & 5.36 \end{bmatrix}$$

satisfying (9). Then, the output funnel controller design is the same as Example 1 in (78)–(80). In Example 2, the design parameters are taken as $c_{i1} = 550$, $c_{i21} = 500$, $c_{i22} = 480$, $a_{il} = 8$, $\ell_{il} = 50$, $\gamma_{il} = 10$, $\zeta_{i1} = 0.9$, $\zeta_{i2} = 0.8$, $\varpi_{i1} = 1500$, $\varpi_{i2} = 1400$, $d_{il} = 0.1$, $\varrho_i = 5$, $\beta = 10$, and $r_{i0} = 0.4$ for $i = 1, 2$ and $l = 1, 2$. Then, it can be obtained by (51) and (52) that $\mu_1 = 3.82$, $v_1 = 20.05$, $\mu_2 = 3.41$, and $v_2 = 30.04$. The parameters of funnels are chosen as $\rho_{it_0} = 2.5$, $\rho_{iT_f} = 0.2$, and $T_f = 1$ for $i = 1, 2$. Based on Theorem 1, it can be concluded that all the signals in the closed-loop system are bounded under a category of switching signals with MDADT satisfying $\tau_{a1} = 0.79 \geq \frac{\ln v_1}{\mu_1}$ and $\tau_{a2} = 1 \geq \frac{\ln v_2}{\mu_2}$.

The initial vectors are provided as $[x_{11}(t_0), x_{12}(t_0), x_{21}(t_0), x_{22}(t_0)]^T = [2, 2, 1.5, 1]^T$, $[\hat{x}_{11}(t_0), \hat{x}_{12}(t_0), \hat{x}_{21}(t_0), \hat{x}_{22}(t_0)]^T = [0.5, 0.8, 0.1, 0.6]^T$, $\hat{\theta}_{11}(t_0) = 5$, $\hat{\theta}_{12}(t_0) = 0.5$, $\hat{\theta}_{21}(t_0) = 1$, $\hat{\theta}_{22}(t_0) = 1$, $\xi_{i1}(t_0) = 0$, $\xi_{i2}(t_0) = 0$, $\varphi_{i11}(t_0) = 0$, and $\varphi_{i12}(t_0) = 0$ for $t_0 \in [-0.2, 0]$. The reference signals are $y_{1r} = 0.4 \sin(2t) + 0.5 \cos(0.5t)$ and $y_{2r} = 0.2 \sin(t) + 0.5 \cos(0.5t)$.

Motivated by [39], for $i = 1, \dots, n$, the following indices are utilized to quantify and compare the performances for

TABLE I
COMPARISON OF INDICES FOR DIFFERENT CONTROL METHODS IN ε_{1y}

Index	IAE ₁	ITAE ₁	ITSE ₁
Proposed Funnel Control	0.0475	0.5546	0.009
Backstepping Control [15]	0.8992	12.2994	0.4421
Dynamic Surface Control [9]	2.7922	37.4556	4.2641

TABLE II
COMPARISON OF INDICES FOR DIFFERENT CONTROL METHODS IN ε_{2y}

Index	IAE ₂	ITAE ₂	ITSE ₂
Proposed Funnel Control	0.0380	0.3986	0.0005
Backstepping Control [15]	0.6814	9.3911	0.2849
Dynamic Surface Control [9]	1.1453	12.7347	0.5860

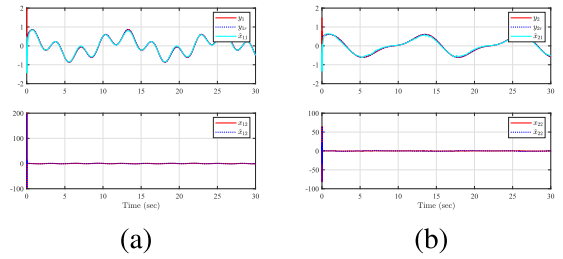


Fig. 8. (a) System output y_1 , reference signal y_{1r} , system state x_{12} , and estimated states \hat{x}_{11} and \hat{x}_{12} ; (b) system output y_2 , reference signal y_{2r} , system state x_{22} , and estimated states \hat{x}_{21} and \hat{x}_{22} (Example 2).

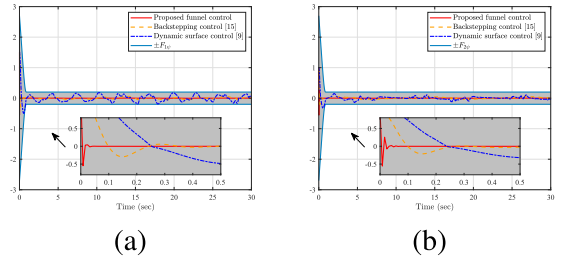


Fig. 9. Output tracking error (a) ε_{1y} and (b) ε_{2y} of the different control strategies in the prespecified performance funnel (Example 2).

the switched nonlinear MIMO-delayed systems under different control methods: 1) Integral absolute errors are defined as $IAE_i = \int_0^\infty |\varepsilon_{iy}(t)| dt$, 2) Integral time-weighted absolute errors are defined as $ITAE_i = \int_0^\infty t |\varepsilon_{iy}(t)| dt$, and 3) Integral time square errors are defined as $ITSE_i = \int_0^\infty t \varepsilon_{iy}^2(t) dt$. In addition, to compare the proposed funnel control with classical control methods (such as the backstepping control [15] and the dynamic surface control [9]), the results of the tracking errors ε_{1y} and ε_{2y} can be given in Tables I and II by using the above indices with the same design parameters and initial conditions, respectively. Simulation results are shown in Figs. 8 – 10 where all signals in the closed-loop system are bounded. The comparison result of the tracking errors ε_{1y} and ε_{2y} of the different control strategies are shown in Fig. 9, respectively. Compared with other control methods, the tracking errors under the proposed funnel control have better transient and steady-state performance with reduced oscillations in the prespecified performance funnels in Fig. 9. Clearly, for the proposed funnel control, the values of errors

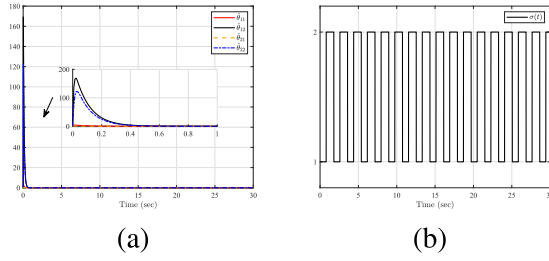


Fig. 10. (a) Adaptive laws $\hat{\theta}_{11}$, $\hat{\theta}_{12}$, $\hat{\theta}_{21}$, and $\hat{\theta}_{22}$; (b) switching signal $\sigma(t)$ (Example 2).

ε_{1y} and ε_{2y} are smaller than those for other control strategies by using the above indices from Tables I and II. Thus, the proposed funnel control method achieves the control performance in the prespecified performance funnels under the category of switching signals with MDADT.

V. CONCLUSION

In this article, an adaptive fuzzy output-feedback funnel control scheme has been presented for a class of switched nonlinear MIMO-delayed systems. By introducing the suitable multiple Lyapunov–Krasovskii functions, all the signals in the closed-loop system are semiglobally uniformly ultimately bounded with a category of switching signals satisfying MDADT via the switched command-filtered-based backstepping techniques. The stability analysis shows the effectiveness and flexibility of the output feedback control scheme. In contrast to the original nonlinear or nondelayed switched systems presented in [7] and [24], the adaptive fuzzy output feedback funnel control approach extends for switched nonlinear MIMO-delayed systems. It is demonstrated that the tracking errors can stay in the prespecified performance funnels under a flexible switching signal with MDADT although the effects of the time-varying delays.

REFERENCES

- [1] D. Cui and Z. Xiang, “Nonsingular fixed-time fault-tolerant fuzzy control for switched uncertain nonlinear systems,” *IEEE Trans. Fuzzy Syst.*, vol. 31, no. 1, pp. 174–183, Jan. 2023.
- [2] J. Zhao and D. J. Hill, “On stability, L_2 -gain and H_∞ control for switched systems,” *Automatica*, vol. 44, pp. 1220–1232, 2008.
- [3] Z. Li, L. Long, and J. Zhao, “Linear output-feedback-based semi-global stabilization for switched nonlinear time-delay systems,” *J. Franklin Inst.*, vol. 356, no. 13, pp. 7224–7245, 2019.
- [4] Z. Liu, J. Yu, and H. K. Lam, “Passivity-based adaptive fuzzy control for stochastic nonlinear switched systems via T-S fuzzy modeling,” *IEEE Trans. Fuzzy Syst.*, vol. 31, no. 4, pp. 1401–1408, Apr. 2023.
- [5] D. Liberzon, *Switching in Systems and Control*. Boston, MA, USA: Birkhäuser, 2003.
- [6] D. Zeng, Z. Liu, C. L. P. Chen, Y. Zhang, and Z. Wu, “Adaptive fuzzy output-feedback predefined-time control of nonlinear switched systems with admissible edge-dependent average dwell time,” *IEEE Trans. Fuzzy Syst.*, vol. 30, no. 12, pp. 5337–5350, Dec. 2022.
- [7] Z. Li, D. Yue, Y. Ma, and J. Zhao, “Neural-networks-based prescribed tracking for nonaffine switched nonlinear time-delay systems,” *IEEE Trans. Cybern.*, vol. 52, no. 7, pp. 6579–6590, Jul. 2022.
- [8] S. Li, C. K. Ahn, and Z. Xiang, “Command-filter-based adaptive fuzzy finite-time control for switched nonlinear systems using state-dependent switching method,” *IEEE Trans. Fuzzy Syst.*, vol. 29, no. 4, pp. 833–845, Apr. 2021.
- [9] B. Niu, J. Kong, X. Zhao, J. Zhang, Z. Wang, and Y. Li, “Event-triggered adaptive output-feedback control of switched stochastic nonlinear systems with actuator failures: A modified MDADT method,” *IEEE Trans. Cybern.*, vol. 53, no. 2, pp. 900–912, Feb. 2023.
- [10] J. Zhang, S. Li, C. K. Ahn, and Z. Xiang, “Decentralized event-triggered adaptive fuzzy control for nonlinear switched large-scale systems with input delay via command-filtered backstepping,” *IEEE Trans. Fuzzy Syst.*, vol. 30, no. 6, pp. 2118–2123, Jun. 2022.
- [11] X. Zhao, L. Zhang, P. Shi, and M. Liu, “Stability and stabilization of switched linear systems with mode-dependent average dwell time,” *IEEE Trans. Autom. Control*, vol. 57, no. 7, pp. 1809–1815, Jul. 2012.
- [12] D. Zhai, A. Y. Lu, J. Dong, and Q. Zhang, “Adaptive tracking control for a class of switched nonlinear systems under asynchronous switching,” *IEEE Trans. Fuzzy Syst.*, vol. 26, no. 3, pp. 1245–1256, Jun. 2018.
- [13] Y. Xie and Q. Ma, “Adaptive event-triggered neural network control for switching nonlinear systems with time delays,” *IEEE Trans. Neural Netw. Learn. Syst.*, vol. 34, no. 2, pp. 729–738, Feb. 2023.
- [14] Z. Li and L. Long, “Global stabilization of switched feedforward nonlinear time-delay systems under asynchronous switching,” *IEEE Trans. Circuits Syst. I: Reg. Papers*, vol. 67, no. 2, pp. 711–724, Feb. 2020.
- [15] L. J. Long and J. Zhao, “Switched-observer-based adaptive neural control of MIMO switched nonlinear systems with unknown control gains,” *IEEE Trans. Neural Netw. Learn. Syst.*, vol. 28, no. 7, pp. 1696–1709, Jul. 2017.
- [16] D. Swaroop, J. K. Hedrick, P. P. Yip, and J. C. Gerdes, “Dynamic surface control for a class of nonlinear systems,” *IEEE Trans. Autom. Control*, vol. 45, no. 10, pp. 1893–1899, Oct. 2000.
- [17] H. Chen, Z. Liu, C. Alippi, B. Huang, and D. Liu, “Explainable intelligent fault diagnosis for nonlinear dynamic systems: From unsupervised to supervised learning,” *IEEE Trans. Neural Netw. Learn. Syst.*, vol. 35, no. 5, pp. 6166–6179, May 2024.
- [18] W. Wu, Z. Peng, D. Wang, L. Liu, and Q. L. Han, “Network-based line-of-sight path tracking of underactuated unmanned surface vehicles with experiment results,” *IEEE Trans. Cybern.*, vol. 52, no. 10, pp. 10937–10947, Oct. 2022.
- [19] Q. Zeng and J. Zhao, “Dynamic event-triggered-based adaptive finite-time neural control for active suspension systems with displacement constraint,” *IEEE Trans. Neural Netw. Learn. Syst.*, vol. 35, no. 3, pp. 4047–4057, Mar. 2024.
- [20] Z. Li, G. Cao, W. Xie, R. Gao, and W. Zhang, “Switched-observer-based adaptive neural networks tracking control for switched nonlinear time-delay systems with actuator saturation,” *Inf. Sci.*, vol. 621, pp. 36–57, 2023.
- [21] X. Xia, J. Pan, T. Zhang, and Y. Fang, “Command filter based adaptive finite-time dynamic surface control for nonlinear systems with unknown input delay under discontinuous input,” *Int. J. Robust Nonlinear Control*, vol. 33, no. 6, pp. 3889–3907, 2023.
- [22] M. Chen, Y. Li, H. Wang, K. Peng, and L. Wu, “Adaptive fixed-time tracking control for nonlinear systems based on finite-time command-filtered backstepping,” *IEEE Trans. Fuzzy Syst.*, vol. 31, no. 5, pp. 1604–1613, May 2023.
- [23] T. Zhang and T. Liu, “Adaptive neural optimal control via command filter for nonlinear multi-agent systems including time-varying output constraints,” *Int. J. Robust Nonlinear Control*, vol. 33, no. 2, pp. 820–849, 2023.
- [24] F. Wang and L. Long, “Switched-observer-based event-triggered adaptive fuzzy funnel control for switched nonlinear systems,” *IEEE Trans. Fuzzy Syst.*, vol. 30, no. 6, pp. 1773–1787, Jun. 2022.
- [25] Y. H. Liu, C. Y. Su, and H. Li, “Adaptive output feedback funnel control of uncertain nonlinear systems with arbitrary relative degree,” *IEEE Trans. Autom. Control*, vol. 66, no. 6, pp. 2854–2860, Jun. 2021.
- [26] R. Ji, D. Li, J. Ma, and S. S. Ge, “Saturation-tolerant prescribed control of MIMO systems with unknown control directions,” *IEEE Trans. Fuzzy Syst.*, vol. 30, no. 12, pp. 5116–5127, Dec. 2022.
- [27] C. P. Bechlioulis and G. A. Rovithakis, “Robust adaptive control of feedback linearizable MIMO nonlinear systems with prescribed performance,” *IEEE Trans. Autom. Control*, vol. 53, no. 9, pp. 2090–2099, Oct. 2008.
- [28] C. Hua, P. Ning, K. Li, and X. Guan, “Fixed-time prescribed tracking control for stochastic nonlinear systems with unknown measurement sensitivity,” *IEEE Trans. Cybern.*, vol. 52, no. 5, pp. 3722–3732, May 2022.
- [29] A. Ilchmann, E. P. Ryan, and C. J. Sangwin, “Tracking with prescribed transient behaviour,” *ESAIM-Control, Optimisation Calculus Variations*, vol. 7, pp. 471–493, 2002.
- [30] C. Liu, H. Wang, X. Liu, and Y. Zhou, “Adaptive finite-time fuzzy funnel control for nonaffine nonlinear systems,” *IEEE Trans. Syst., Man, Cybern. Syst.*, vol. 51, no. 5, pp. 2894–2903, May 2021.
- [31] H. K. Lam, C. Liu, L. Wu, and X. Zhao, “Polynomial fuzzy-model-based control systems: Stability analysis via approximated membership functions considering sector nonlinearity of control input,” *IEEE Trans. Fuzzy Syst.*, vol. 23, no. 6, pp. 2202–2214, Dec. 2015.

- [32] Y. Li, K. Li, and S. Tong, "An observer-based fuzzy adaptive consensus control method for nonlinear multiagent systems," *IEEE Trans. Fuzzy Syst.*, vol. 30, no. 11, pp. 4667–4678, Nov. 2022.
- [33] S. I. Han and J. M. Lee, "Fuzzy echo state neural networks and funnel dynamic surface control for prescribed performance of a nonlinear dynamic system," *IEEE Trans. Ind. Electron.*, vol. 61, no. 2, pp. 1099–1112, Feb. 2014.
- [34] M. Van, S. S. Ge, and H. Ren, "Finite time fault tolerant control for robot manipulators using time delay estimation and continuous nonsingular fast terminal sliding mode control," *IEEE Trans. Cybern.*, vol. 47, no. 7, pp. 1681–1693, Jul. 2017.
- [35] J. A. Farrell, M. Polycarpou, M. Sharma, and W. Dong, "Command filtered backstepping," *IEEE Trans. Autom. Control*, vol. 54, no. 6, pp. 1391–1395, Jun. 2009.
- [36] Z. Li, H. Chen, W. Wu, and W. Zhang, "Dynamic output feedback fault-tolerant control for switched vehicle active suspension delayed systems," *IEEE Trans. Veh. Technol.*, early access, Feb. 27, 2024, doi: [10.1109/TVT.2024.3370094](https://doi.org/10.1109/TVT.2024.3370094).
- [37] L. Long and Y. Bian, "State constraints-based adaptive neural network control for switched nonlinear systems with unmodeled dynamics," *Int. J. Robust Nonlinear Control*, vol. 30, no. 18, pp. 7835–7856, 2020.
- [38] H. J. Estrada-García, L. A. Márquez-Martínez, and C. H. Moog, "Master-slave synchronization for two inverted pendulums with communication time-delay," in *Topics in Time Delay Systems: Analysis, Algorithms and Control*. Berlin, Germany: Springer, 2009, pp. 403–413.
- [39] J. Na, Y. Huang, X. Wu, Y. J. Liu, Y. Li, and G. Li, "Active suspension control of quarter-car system with experimental validation," *IEEE Trans. Syst., Man, Cybern. Syst.*, vol. 52, no. 8, pp. 4714–4726, Aug. 2022.



Zhenhua Li received the B.S. degree in automation from the Harbin University of Science and Technology, Harbin, China, in 2017, and the M.S. degree in control theory and control engineering from Northeastern University, Shenyang, China, in 2020. He is currently working toward the Eng.D. degree in electronic information with the Department of Automation, Shanghai Jiao Tong University, Shanghai, China.

His research interests include adaptive control, nonlinear systems, observer theory, switched systems, time-delay systems, and autonomous systems.

Dr. Li was the recipient of the Best Theory Paper Award at the China Automation Congress from Chinese Association of Automation (CAA) in 2022. He is a Reviewer of some international journals, such as IEEE TRANSACTIONS ON INDUSTRIAL INFORMATICS and *International Journal of Systems Science*.



Hongtian Chen (Member, IEEE) received the Ph.D. degree in control theory and control engineering from the College of Automation Engineering, Nanjing University of Aeronautics and Astronautics, Nanjing, China, in 2019.

From 2019 to 2023, he was a Postdoctoral Fellow with the University of Alberta, Edmonton, AB, Canada. Since 2023, he has been an Associate Professor with the Department of Automation, Shanghai Jiao Tong University, Shanghai, China. His research interests include fault diagnosis and fault-tolerant

control, data mining and analytics, machine learning, and cooperative control; and their applications in high-speed trains, new energy systems, industrial processes, and autonomous systems.

Dr. Chen was the recipient of the Grand Prize of Innovation Award of Ministry of Industry and Information Technology of the People's Republic of China in 2019, the Excellent Ph.D. Thesis Award of Jiangsu in 2020, the Excellent Doctoral Dissertation Award from Chinese Association of Automation in 2020, Marie Skłodowska-Curie Actions in 2023, and Pujiang Scholar in 2023. He is an Associate Editor and Guest Editor of several international journals, such as IEEE TRANSACTIONS ON INSTRUMENTATION AND MEASUREMENT, IEEE TRANSACTIONS ON ARTIFICIAL INTELLIGENCE, IEEE TRANSACTIONS ON NEURAL NETWORKS AND LEARNING SYSTEMS, and *International Journal of Robotics and Automation*. He was also a Co-Chair and Program Chair for international conferences, such as the 6th International Conference on Robotics, Control, and Automation Engineering.



Hak-Keung Lam (Fellow, IEEE) received the B.Eng. (Hons.) and Ph.D. degrees in electronic and information engineering from the Hong Kong Polytechnic University, Hong Kong, in 1995 and 2000, respectively.

He was with the Department of Electronic and Information Engineering, the Hong Kong Polytechnic University, as a Postdoctoral Fellow, in 2000, and then as a Research Fellow, in 2005. In 2005, he joined as a Lecturer with King's College London, London, U.K., where he is currently a Reader. He has coedited two

edited volumes: *Control of Chaotic Nonlinear Circuits* (World Scientific, 2009) and *Computational Intelligence and Its Applications* (World Scientific, 2012); and authored or coauthored three monographs: *Stability Analysis of Fuzzy-Model-Based Control Systems* (Springer, 2011), *Polynomial Fuzzy Model-Based Control Systems* (Springer, 2016), and *Analysis and Synthesis for Interval Type-2 Fuzzy-Model-Based Systems* (Springer, 2016). His research interests include intelligent control, computational intelligence, and machine learning.

Dr. Lam was an Associate Editor for IEEE TRANSACTIONS ON CIRCUITS AND SYSTEMS—II: EXPRESS BRIEFS and is an Associate Editor for IEEE TRANSACTIONS ON FUZZY SYSTEMS, *IET Control Theory and Applications*, *International Journal of Fuzzy Systems*, *Neurocomputing*, and *Nonlinear Dynamics*. He is a Guest Editor for a number of international journals. He was a Program Committee Member, International Advisory Board Member, Invited Session Chair, and Publication Chair for various international conferences and a reviewer for various books, international journals, and international conferences. He is on the editorial boards of *Journal of Intelligent Learning Systems and Applications*, *Journal of Applied Mathematics*, *Mathematical Problems in Engineering*, *Modeling and Simulation in Engineering*, *Annual Review of Chaos Theory*, *Bifurcations and Dynamical System*, *The Open Cybernetics and Systemics Journal*, *Cogent Engineering*, and *International Journal of Sensors, Wireless Communications and Control*. He was named as a highly cited Researcher.



Wentao Wu (Student Member, IEEE) received the B.E. degree in electrical engineering and automation from the Harbin University of Science and Technology, Harbin, China, in 2018, and the M.E. degree in electrical engineering from Dalian Maritime University, Dalian, China, in 2021. He is currently working toward the Ph.D. degree in electronic information from Shanghai Jiao Tong University, Shanghai, China.

From 2023 to 2024, he was a Visiting Research Scholar with the Department of Mechanical Engineering, University of Victoria, Victoria, BC, Canada. His current research interests include cooperative control, safety-critical control, constrained control, and game-based control of multiple marine vehicles.



Weidong Zhang (Senior Member, IEEE) received the B.S. degree in measurement technology and instruments, M.S. degree in applied electronic technology, and Ph.D. degree in control theory and its application from Zhejiang University, Hangzhou, China, in 1990, 1993, and 1996, respectively.

He was a Postdoctoral Fellow with Shanghai Jiao Tong University, Shanghai, China, where he joined as an Associate Professor in 1998, and has been a Full Professor since 1999. From 2003 to 2004, he was an Alexander von Humboldt Fellow with the University of Stuttgart, Stuttgart, Germany. From 2013 to 2017, he was a Deputy Dean with the Department of Automation, Shanghai Jiao Tong University. He is currently a Director of the Engineering Research Center of Marine Automation, Shanghai Municipal Education Commission, and Director of Marine Intelligent System Engineering Research Center, Ministry of Education, China. He has authored or coauthored more than 300 papers and one book. His research interests include control theory, machine learning theory, and their applications in industry and autonomous systems.

Dr. Zhang was the recipient of National Science Fund for Distinguished Young Scholars, China, and Cheung Kong Scholar, Ministry of Education, China. He has been recognized as an Elsevier's Most Cited Researcher.